Pramāṇa, Vol. 11, No. 3, September 1978, pp. 251–288, © printed in India

Inelastic neutron scattering from and lattice dynamics of α-KNO_3

K R RAO, S L CHAPLOT, P K IYENGAR, A H VENKATESH and P R VIJAYARAGHAVAN
Nuclear Physics Division, Bhabha Atomic Research Centre, Bombay 400 085

MS received 17 April 1978; revised 3 July 1978

Abstract. Coherent inelastic neutron scattering techniques are employed to measure several branches of the phonon dispersion relation in KNO_3 in its orthorhombic (α-phase or phase II) form at room temperature. Group theoretical selection rules for external modes of the crystal have been used in the measurements along the three symmetry directions $\Sigma(\xi 00)$, $\Delta(0\xi 0)$ and $\Lambda(00\xi)$.

Theoretical investigation of the lattice dynamics of the crystal is carried out on the basis of a rigid molecular-ion model using the external mode formalism. A two-body potential consisting of the Coulombic interaction and the Born-Mayer type short range interaction is assumed. The effective charges and radii of different atoms are determined by applying the stability criterion for the crystal. Dispersion curves are calculated, representation by representation, making use of group theoretical information. Comparison of theoretical results with experimental information on elastic constants, optical data and neutron results are made. Agreement between theoretical and the various experimental results may be considered very satisfactory.

Keywords. Lattice dynamics; potassium nitrate; inelastic neutron scattering; neutron scattering selection rules; group theoretical analysis.

1. Introduction

KNO_3 (potassium nitrate) is an interesting solid because of its ferroelectric properties in one of its phases (Jona and Shirane 1962). The possibility of using this material as a fast, non-volatile, non-destructive read out memory element has been suggested in the literature (Born *et al* 1970). Its switching behaviour has been studied by several workers (Dork *et al* 1964; Nolta *et al* 1965). The nature of ferroelectricity in KNO_3, the underlying phenomenon for these properties, has been extensively investigated (Nolta and Schubring 1962; Chen and Chernow 1967, Siouffi and Cerisier 1972, Teng *et al* 1971; Yanagi and Sawada 1963; Gay 1967). In addition other properties like morphology, crystallisation, structure (Shinnaka 1962, Gay 1967; Teng 1970 and Nimmo and Lucas 1973), dielectric constant (Sawada *et al* 1961; Doucet *et al* 1965; Yanagi 1965; Mansingh and Smith 1971), etc are known. Perhaps because of the simple structure in the ferroelectric phase, lattice dynamics of this phase is also theoretically investigated earlier (Krishnan and Haridasan 1972).

It is now well understood that there is a close relation between phase transitions and lattice dynamics (Cochran 1972). In particular, displacive phase transitions in ionic crystals are responsible for onset of ferroelectricity in a number of crystals. From the point of view of understanding the mechanism of phase transitions in solids it is desirable to study the lattice dynamics of various phases.

The objective of this paper is to present results of our experimental and theoretical investigations of the lattice dynamics of the room temperature phase of KNO_3. Details of the phase diagram and structure are given in section 2. We have carried out neutron inelastic scattering experiments on a single crystal of KNO_3 and measured the phonon dispersion curves. Since there are four molecules per unit cell (20 atoms per cell), a very large number of phonon branches (as many as 60) may be responsible for the inelastic processes. However one can treat the NO_3^- ion as a rigid unit (sometimes referred to as ' molecule ') capable of translations and rotations only as is indicated in section 3. Thereby one can invoke the external mode formalism. In section 4 we discuss the role of group theoretical selection rules for neutron scattering, particularly for the choice of suitable regions of reciprocal space, to make meaningful experiments. Experimental aspects are covered in section 5. We have resorted to a simple lattice dynamical model to carry out theoretical calculation of the dispersion relation of phonons. This model treats the dynamics of the crystals in the spirit of the conventional rigid ion model wherein one does not take into account the polarisabilities of any of the ions; but we are essentially concerned with the ' external ' modes of the lattice (Venkataraman and Sahni 1970). The external mode formalism has been used with several crystals like hexamine (Dolling and Powell 1970), $NaNO_2$ (Sakurai *et al* 1970), Boron trihalides (Binbreck *et al* 1974), etc. In some of these studies the ionic nature of the ' molecular ' constituents is taken into account as point charges and detailed charge distribution in the ' molecule ' is not considered. One of the important aspects of the work of Venkataraman and Sahni (1970) is the extension of Kellermann's work to external modes by considering detailed charge distribution in ' molecules'. Although this formalism applicable for *ionic* crystals has been existing in literature for nearly a decade, to the best of our knowledge it has not been used and our work is perhaps the first to make use of this aspect by considering in detail the various Coulomb coefficients of ' *molecular* ' units. The details of the dynamical equations are given in section 6. Group theoretical aspects which help to considerably simplify the problem are also discussed here. Section 7 goes into details of two models investigated. Certain constraints on the crystal potential are discussed which lead to determination of potential parameters. Application of theoretical aspects given in sections 6 and 7 to the case of α-KNO_3 are discussed in section 8. Comparison of theoretical and experimental results on elastic constants, optical data and the present neutron results is made in section 9. Section 10 gives summary of results of our study.

2. Structure

2.1. *General*

KNO_3 exhibits several polymorphic transitions, as summarised in the phase diagram given in figure 1. Figure 1a indicates the pressure vs temperature diagram (Rapoport and Kennedy 1965) and figure 1b the appearances of various phases at atmospheric pressure as a function of temperature, on heating and cooling. The crystallographic information is summarised in figure 1c. In the temperature range 124°C to 110°C by cooling from higher temperature, the crystal exhibits the ferroelectric phase, commonly referred to as the γ-phase or phase III. The high temperature phase

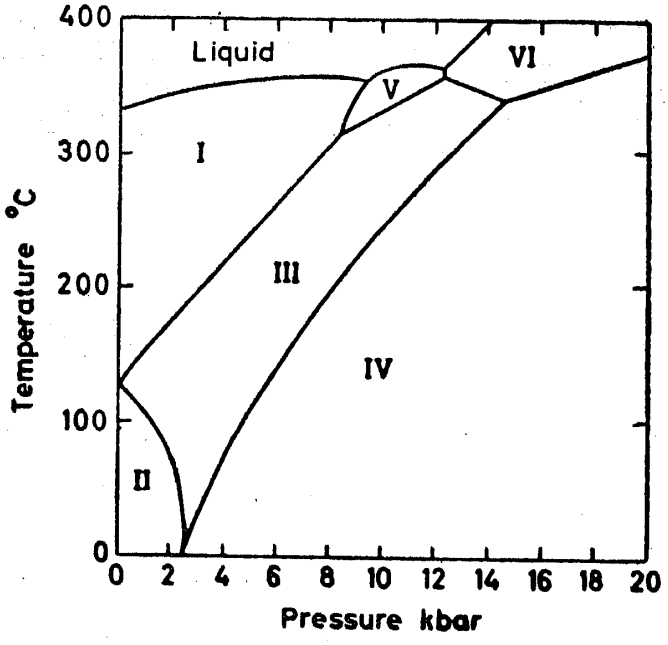

(a)

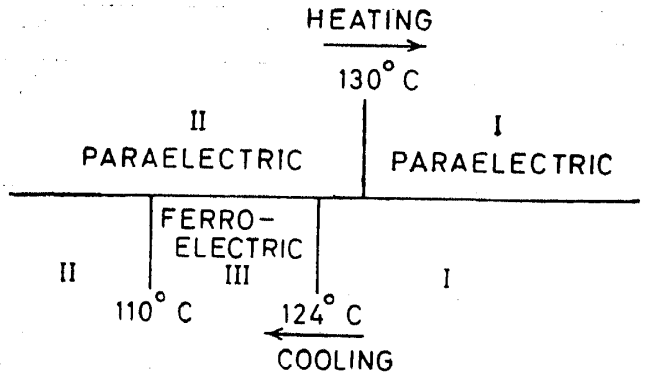

(b)

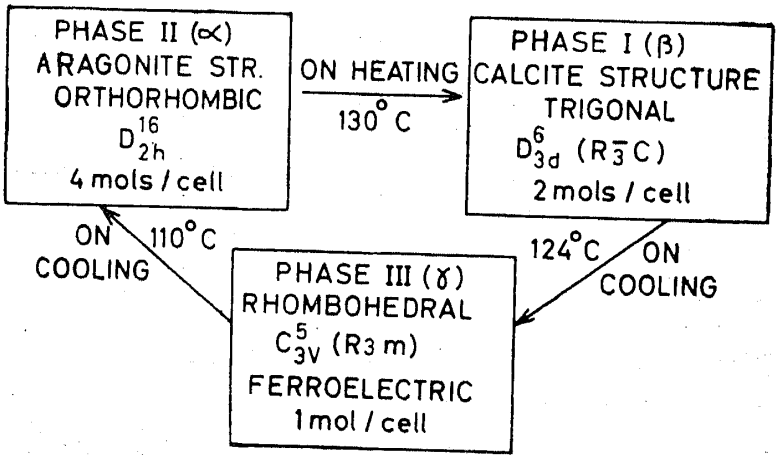

(c)

Figure 1. Phase diagram of KNO_3. **a.** Pressure vs temperature diagram. **b.** Phases at atmospheric pressure in the heating and cooling cycles. **c.** Crystallographic information in various phases.

above 130°C is generally referred to as β-phase or phase I. This phase can be supercooled down to 124° and is metastable in the 130°C to 124°C range. The room temperature phase with which we are concerned is generally referred to as α-phase or phase II. It may be noted that the crystal transforms itself from α-phase directly to γ-phase under pressure.

2.2 *The α-phase*

In the α-phase, having the space group D_{2h}^{16}, the unit cell is simple orthorhombic and contains four molecules. The crystal structure was studied by Edwards (1931) by x-ray diffraction. The arrangement of atoms was found to be isomorphous with the well known structure proposed by Bragg (1924) and Wyckoff (1925) for aragonite. Recently Nimmo and Lucas (1973) have reinvestigated the crystal structure by neutron diffraction. Among other results, they find that the fractional z-coordinate of potassium and the fractional y-coordinate of nitrogen does not have special and equal values of 0·75. The cell parameters and fractional coordinates are given in

Table 1a. Cell dimensions and fractional coordinates of atomic positions in α-KNO

(i) *Cell Dimensions* (Å):

	a	b	c	Reference
1	6·45	5·43	9·17	Edwards (1931)
2	6·4309	5·4142	9·1659	Wyckoff (1964)
3	6·4213	5·4119	9·1567	Nimmo and Lucas (1973)
4	6·4255	5·4175	9·1709	Wyckoff (Vol II)

(ii) *Fractional coordinates of atomic positions*:

	Atom	ξ	η	ζ	Reference
1	K	0·75	0·25	0·416	Slater (1965)
	N	0·417	0·25	0·75	
	O(1)	0·417	0·25	0·617	
	O(2)	0·417	0·444	0·814	
2	K	0·75	0·25	0·416	Edwards (1931)
	N	−0·083	0·25	0·750	
	O(1)	−0·083	0·25	0·883	
	O(2)	−0·083	0·444	0·686	
3	K	0·7568	0·2500	0·4166	Nimmo and Lucas (1973)
	N	−0·0848	0·2500	0·7548	
	O(1)	−0·0893	0·2500	0·8902	
	O(2)	−0·0849	0·4492	0·6866	

Table 1b. Atomic masses and scattering amplitudes:

Atom	Atomic mass (amu)	Neutron scattering amplitude (10^{-12} cm)
K	39·1	0·35
N	14·0	0·94
O	16·0	0·581

Table 1c. ' Molecular ' labelling and atomic positions fractional coordinates as per Slater (1965) and cell dimensions as per Wyckoff (Vol. II)

Molecule No.	Atom No.	Atom	Fractional coordinates			Coordinates (A)		
			ξ	η	ζ	x	y	z
1	1	K	0·75	0·25	0·416	4·8191	1·3544	3·8151
2	1	K	0·25	0·75	0·584	1·6064	4·0631	5·3558
3	1	K	0·25	0·25	0·084	1·6064	1·3544	0·7704
4	1	K	0·75	0·75	0·916	4·8191	4·0631	8·4005
5	1	N	0·417	0·25	0·75	2·6794	1·3544	6·8782
	2	O	0·417	0·25	0·617	2·6794	1·3544	5·6584
	3	O	0·417	0·444	0·814	2·6794	2·4054	7·4651
	4	O	0·417	0·056	0·814	2·6794	0·3034	7·4651
6	1	N	0·583	0·75	0·25	3·7461	4·0631	2·2927
	2	O	0·583	0·75	0·383	3·7461	4·0631	3·5125
	3	O	0·583	0·944	0·186	3·7461	5·1141	1·7058
	4	O	0·583	0·556	0·186	3·7461	3·0121	1·7058
7	1	N	0·917	0·25	0·75	5·8922	1·3544	6·8782
	2	O	0·917	0·25	0·883	5·8922	1·3544	8·0979
	3	O	0·917	0·056	0·686	5·8922	0·3034	6·2912
	4	O	0·917	0·444	0·686	5·8922	2·4054	6·2912
8	1	N	0·083	0·75	0·25	0·5333	4·0631	2·2927
	2	O	0·083	0·75	0·117	0·5333	4·0631	1·0730
	3	O	0·083	0·556	0·314	0·5333	3·0121	2·8797
	4	O	0·083	0·944	0·314	0·5333	5·1141	2·8797

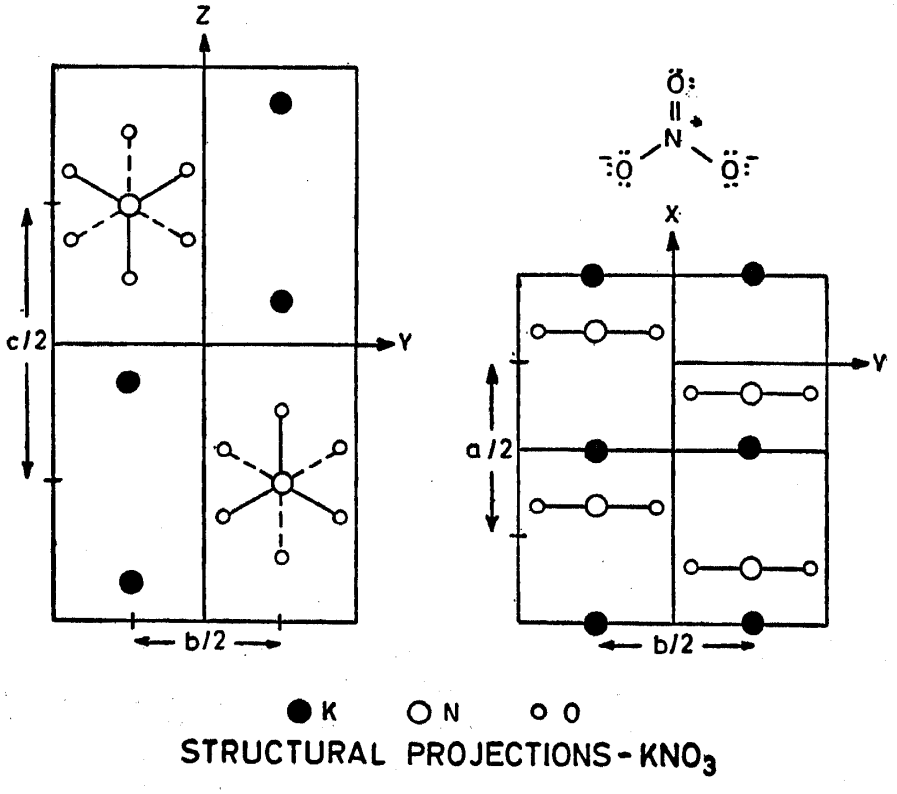

Figure 2. Projection of atomic coordinates on the xy and yz planes. The inset shows the configuration of the NO_3^- ion according to Pauling (1967).

Table 2. Space group operations of D_{2h}^{16}

Symmetry operation	Seitz's notation	International tables	Kovalev	S	v(S)
S_1	$\{E \mid 0\}$	(xyz)	$(h_1 \mid 0)$	$\begin{bmatrix}1&0&0\\0&1&0\\0&0&1\end{bmatrix}$	0
S_2	$\{C_2(x)/\mathbf{v}_1\}$	$(x+\frac{1}{2}, -y+\frac{1}{2}, -z+\frac{1}{2})$	$(h_2 \mid \mathbf{v}_1)$	$\begin{bmatrix}1&0&0\\0&-1&0\\0&0&-1\end{bmatrix}$	$\begin{bmatrix}\frac{1}{2}\\\frac{1}{2}\\\frac{1}{2}\end{bmatrix}$
S_3	$\{C_2(y) \mid \mathbf{v}_2\}$	$(-x, y+\frac{1}{2}, -z)$	$(h_3 \mid \mathbf{v}_2)$	$\begin{bmatrix}-1&0&0\\0&1&0\\0&0&-1\end{bmatrix}$	$\begin{bmatrix}0\\\frac{1}{2}\\0\end{bmatrix}$
S_4	$\{C_2(z) \mid \mathbf{v}_3\}$	$(-x+\frac{1}{2}, -y, z+\frac{1}{2})$	$(h_4 \mid \mathbf{v}_3)$	$\begin{bmatrix}-1&0&0\\0&-1&0\\0&0&+1\end{bmatrix}$	$\begin{bmatrix}\frac{1}{2}\\0\\\frac{1}{2}\end{bmatrix}$
S_5	$\{i \mid 0\}$	$(-x, -y, -z)$	$(h_{25} \mid 0)$	$\begin{bmatrix}-1&0&0\\0&-1&0\\0&0&-1\end{bmatrix}$	0
S_6	$\{\sigma_x \mid \mathbf{v}_1\}$	$(-x+\frac{1}{2}, y+\frac{1}{2}, z+\frac{1}{2})$	$(h_{26} \mid \mathbf{v}_1)$	$\begin{bmatrix}-1&0&0\\0&1&0\\0&0&1\end{bmatrix}$	$\begin{bmatrix}\frac{1}{2}\\\frac{1}{2}\\\frac{1}{2}\end{bmatrix}$
S_7	$\{\sigma_y \mid \mathbf{v}_2\}$	$(x, -y+\frac{1}{2}, z)$	$(h_{27} \mid \mathbf{v}_2)$	$\begin{bmatrix}1&0&0\\0&-1&0\\0&0&1\end{bmatrix}$	$\begin{bmatrix}0\\\frac{1}{2}\\0\end{bmatrix}$
S_8	$\{\sigma_z \mid \mathbf{v}_3\}$	$(x+\frac{1}{2}, y, -z+\frac{1}{2})$	$(h_{28} \mid \mathbf{v}_3)$	$\begin{bmatrix}1&0&0\\0&1&0\\0&0&-1\end{bmatrix}$	$\begin{bmatrix}\frac{1}{2}\\0\\\frac{1}{2}\end{bmatrix}$

$\mathbf{v}_1 = \frac{1}{2}a\mathbf{i}+\frac{1}{2}b\mathbf{j}+\frac{1}{2}c\mathbf{k}$
$\mathbf{v}_2 = \frac{1}{2}b\mathbf{j}$
$\mathbf{v}_3 = \frac{1}{2}a\mathbf{i}+\frac{1}{2}c\mathbf{k}$

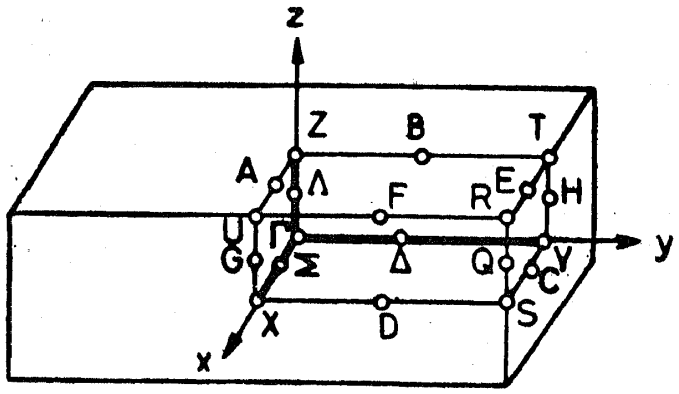

Figure 3. Brillouin zone of the orthorhombic lattice.

table 1a. We have used the cell parameters given by Wyckoff (1964) and fractional coordinates given by Slater (1965) in this paper.

Given the fractional coordinates, one can describe the disposition of atoms in the cell as follows: The potassiums, the nitrogens and one set of oxygens (0(1)) are at $\pm(a\,\xi\,\mathbf{i},\ b\,\eta\,\mathbf{j},\ c\,\zeta\,\mathbf{k})$ and $\pm((\frac{1}{2}+\xi)\,a\,\mathbf{i},\ b\,\eta\,\mathbf{j},\ (\frac{1}{2}-\zeta)\,c\,\mathbf{k})$ and the other set of oxygens (0(2)) are at $(a\,\xi\,\mathbf{i},\ b\,\eta\,\mathbf{j},\ c\,\zeta\,\mathbf{k})$ and at positions derived from this position

by operations of the point group of the lattice. **i**, **j** and **k** are unit vectors along a, b and c cell axes. The atom positions in the unit cell are given in table 1c. The space group operations of D_{2h}^{16} are given in table 2. Figure 2 shows the projections of the coordinates of the atoms in the unit cell in the xy and yz planes.

2.3 *Brillouin zone*

The Brillouin zone of the simple orthorhombic lattice which is also orthorhombic is shown in figure 3. The nomenclature of symmetry points and lines follows Slater (1965). Our measurements are confined to the symmetry directions Σ, Δ, and Λ.

3. The external mode approach in the dynamics of KNO_3

Bonding inside NO_3^- ion in KNO_3 is much stronger than the bonding between any two different ions in the lattice. This is substantiated by the fact that the internal modes (covalent modes) of NO_3^- ions correspond to high frequencies as given in table 3. These modes do not change significantly through different phases of the system. One can therefore resort to 'external' mode approach (Venkataraman and Sahni 1970) to deal with lattice dynamics of KNO_3. In this approach the NO_3^- ion is assumed to be a rigid unit capable of rotation and translation as a whole. The approximation of rigidity of ionic units and separation of external modes from internal modes is based on the fact that internal mode frequencies are well separated from external mode frequencies and consequently there is no coupling between the two types of modes.

Table 3. Internal modes of KNO_3 (Balkanski *et al*, 1969)

Observed frequencies (cm^{-1}) in		
Phase I(β)	Phase II (α)	Phase III (γ)
714	714	716, 717
836	829, 830	836
1056	1054	1053, 1054
1428	1348, 1362	1352

4. One phonon neutron scattering in complex crystals

4.1 *One phonon cross section*

Determination of dispersion relation $\nu_j(\mathbf{q})$, the frequency-wave vector relation (ν_j is the frequency of the jth branch for a wave vector $\mathbf{q}$) of a complex crystal is an intricate problem because of the large number of branches associated. If there are μ atoms and ν 'molecules' in the unit cell, there would be as many as $3\mu+6\nu$ external modes all of which could, in principle, contribute to any inelastic scattering process corresponding to a given wave vector. The problem of identifying the branches becomes therefore formidable as n, the number of constituents ($=\mu+\nu$) becomes very large. The number of external modes would be less than $3\mu+6\nu$ if a few of the branches were to degenerate by symmetry.

The one phonon (inelastic) coherent scattering cross-section per unit cell is given by,

$$\frac{d^2\sigma}{d\Omega d\epsilon} = (k_f/k_i)\{\hbar(n_{\mathbf{q}j}\pm\tfrac{1}{2}+\tfrac{1}{2})/(2\omega_j(\mathbf{q})\,|J_j(\omega)|)\}$$

$$\times |F_j(\mathbf{Q})|^2\,\delta(\mathbf{Q}-2\pi\tau-\mathbf{q})\,\delta(\epsilon\pm\hbar\omega_j(\mathbf{q}) \tag{1}$$

with the population factor

$$n_{\mathbf{q}j} = \{\exp(\hbar\omega_j(\mathbf{q})/(k_BT))-1\}^{-1} \tag{2}$$

the inelastic (dynamical) structure factor for the ' atomic ' model of the crystal,

$$F_j(\mathbf{Q}) = \sum_k (b_k/M_k^{1/2})\{\mathbf{Q}\cdot\mathbf{e}_k(\mathbf{q}\,j)\}\exp(-W_k(\mathbf{Q})\exp(2\pi i\,\mathbf{G}\cdot\mathbf{r}_k) \tag{3}$$

and the Jacobian,

$$J_j(\omega) = \{1\pm(m/(\hbar\,\mathbf{k}_f^2))k_f\cdot\nabla_q\,\omega_j(\mathbf{q})\}^{-1} \tag{4}$$

Here b_k is the bound-atom coherent scattering amplitude of kth nucleus, $\mathbf{r}_k$ the position vector of the kth nucleus, M_k its mass and $\exp(-W_k(\mathbf{Q}))$ its Debye-Waller factor. m is the neutron mass and $\mathbf{k}_i$ and $\mathbf{k}_f$ are incident and scattered neutron wave vectors respectively. $\mathbf{Q}=\mathbf{k}_i-\mathbf{k}_f$ is the wave vector transfer and $\mathbf{G}$ a reciprocal lattice vector. $\epsilon(=\hbar\omega)$ is the neutron energy transfer, $\hbar$ is Planck's constant and k_B the Boltzmann's constant. $\mathbf{e}_k(\mathbf{q}\,j)$ is the polarisation vector of the kth nucleus when its displacement is governed by a phonon $\omega_j(\mathbf{q})$. The + and − sign in (1) and (4) are associated with phonon creation (neutron energy loss) and phonon annihilation (neutron energy gain) respectively.

In the external mode formalism, the dynamical structure factor $F_j(\mathbf{Q})$ given in (3) is replaced by an involved expression (Casella and Trevino 1972, their eq. (67)) containing translational and rotational components. Further details are given in the next section.

4.2 *Group theoretical selection rules for neutron scattering*

Elliot and Thorpe (1967) discussed the properties of the symmetry vectors and derived a sum rule for the dynamical structure factor. They showed that the sum of squares of the reduced structure factor (i.e. the dynamical structure factor modulo $\mathbf{Q}^2\exp(-2W_k(\mathbf{Q}))\{\hat{\mathbf{Q}}\cdot\hat{\mathbf{e}}_k(\mathbf{q}\,j)\}^2$) at any point $\mathbf{Q}$ over the modes j which transform according to the same row λ of an irreducible multiplier representation (IMR) s of the group of the wave vector $\mathbf{q}$, $(G_0(\mathbf{q}))$ is constant and completely determined by symmetry, that is by the matrix elements of the IMR:

$$F^s(\mathbf{Q}) = \sum_{j\in s\lambda} |F_j(\mathbf{Q})|^2 = C_{s\lambda}(\mathbf{Q}) \tag{5}$$

The sum rule, which is sometimes referred to as ' selection rule ', is an important aid in analysing intensities in one phonon scattering, in assigning observed phonons to different symmetries and in identifying regions of the reciprocal space where phonons of the different symmetries may contribute to considerable inelastic cross-section.

The formalism developed by Elliot and Thorpe (1967) is strictly applicable to ' atomic ' case. Recently, Casella and Trevino (1972) have studied the nature of sum rules governing external modes only. They have shown that the structure factor $F^s(\mathbf{Q})$ associated with IMR s can be written as

$$F^s(\mathbf{Q}) = F_T^s(\mathbf{Q}) + F_R^s(\mathbf{Q})$$

where $F_T^s(\mathbf{Q})$ is associated with translations of atomic and ' molecular ' centres of mass and $F_R^s(\mathbf{Q})$ with rotations about centre of mass of 'molecules'. The detailed formalism has been used only in a few cases so far, namely for study of dynamics of $NaNO_3$ (Trevino *et al* 1974) and of D_2O_2 (Trevino *et al* 1976). Trevino and Casella (private communication) have developed the software for calculating $F_T^s(\mathbf{Q})$ and $F_R^s(\mathbf{Q})$. We have employed this software to obtain the structure factors. We have also cross-checked the results of the software by using a small program developed by us to calculate the sum rule for $F^s(\mathbf{Q})$ in external mode approach.

The input to the software (Trevino and Casella, private communication) include atomic (molecular) coordinates, atomic masses and scattering amplitudes (table 1b), matrix representations of rotational operations (table 2) and the IMR corresponding to $G_0(\mathbf{q})$ of $\mathbf{q}$ (see table 4a) under consideration. In table 5 we give $F_T^s(\mathbf{Q})$ and $F_R^s(\mathbf{Q})$ for $\mathbf{q}$ along Λ direction at a few lattice points. From this table we see that at $\mathbf{G}=(050)$,

Table 4. (a) $G_0(\mathbf{q})$ for Σ, Δ, Λ directions and their irreducible representations (Kovalev 1964) $\tau^s(\mathbf{q}, R)$

Σ $(\xi\ 0\ 0)$	$G_0(\Sigma)$:	h_1	h_2	h_{27}	h_{28}
Δ $(0\ \xi\ 0)$	$G_0(\Delta)$:	h_1	h_3	h_{26}	h_{28}
Λ $(0\ 0\ \xi)$	$G_0(\Lambda)$:	h_1	h_4	h_{26}	h_{27}

Representation	IMRs			
$\Sigma_1\ \Delta_1\ \Lambda_1$	1	1	1	1
$\Sigma_2\ \Delta_2\ \Lambda_2$	1	1	−1	−1
$\Sigma_3\ \Delta_3\ \Lambda_3$	1	−1	1	−1
$\Sigma_4\ \Delta_4\ \Lambda_4$	1	−1	−1	1

$-\frac{1}{2}<\xi<\frac{1}{2}$

(b) Decomposition of $T(\mathbf{q})$:

$$T(\Sigma) = 10\Sigma_1 + 8\Sigma_2 + 10\Sigma_3 + 8\Sigma_4$$
$$T(\Delta) = 9\Delta_1 + 9\Delta_2 + 9\Delta_3 + 9\Delta_4$$
$$T(\Lambda) = 10\Lambda_1 + 8\Lambda_2 + 8\Lambda_3 + 10\Lambda_4$$

(c) Compatibility relations

$$\Sigma_1 + \Sigma_3 \rightarrow X_1$$
$$\Sigma_2 + \Sigma_4 \rightarrow X_2$$
$$\Delta_1 + \Delta_4 \rightarrow Y_1$$
$$\Delta_2 + \Delta_3 \rightarrow Y_2$$
$$\Lambda_1 + \Lambda_4 \rightarrow Z_4$$
$$\Lambda_2 + \Lambda_3 \rightarrow Z_3$$

Table 5. Neutron inelastic structure factors $F_T^S(Q)$ and $F_R^S(Q)$ for some typical wave vectors of **q** along $\Lambda(00\xi)$ direction at certain reciprocal lattice vectors **G**

G	$\xi\left(\frac{cq}{2\pi}\right)$	$F_T^{\Lambda_1}$	$F_R^{\Lambda_1}$	$F_T^{\Lambda_2}$	$F_R^{\Lambda_2}$	$F_T^{\Lambda_3}$	$F_R^{\Lambda_3}$	$F_T^{\Lambda_4}$	$F_R^{\Lambda_4}$
(0 5 0)	0·2	0·00	0·00	15·53	0·06	0·00	0·00	0·03	0·00
	0·4	0·00	0·00	15·14	0·24	0·00	0·00	0·06	0·00
(0 6 0)	−0·4	0·05	0·00	0·00	0·00	14·25	0·39	0·00	0·00
	−0·2	0·04	0·00	0·00	0·00	14·62	0·31	0·00	0·00
(6 0 0)	0·2	0·11	0·00	0·00	0·00	0·00	0·00	16·05	0·12
	0·4	0·10	0·00	0·00	0·00	0·00	0·00	15·30	0·11
(6 0 1)	−0·4	14·98	1·01	0·00	0·00	0·00	0·00	0·17	0·01
	−0·2	14·10	1·73	0·00	0·00	0·00	0·00	0·21	0·01

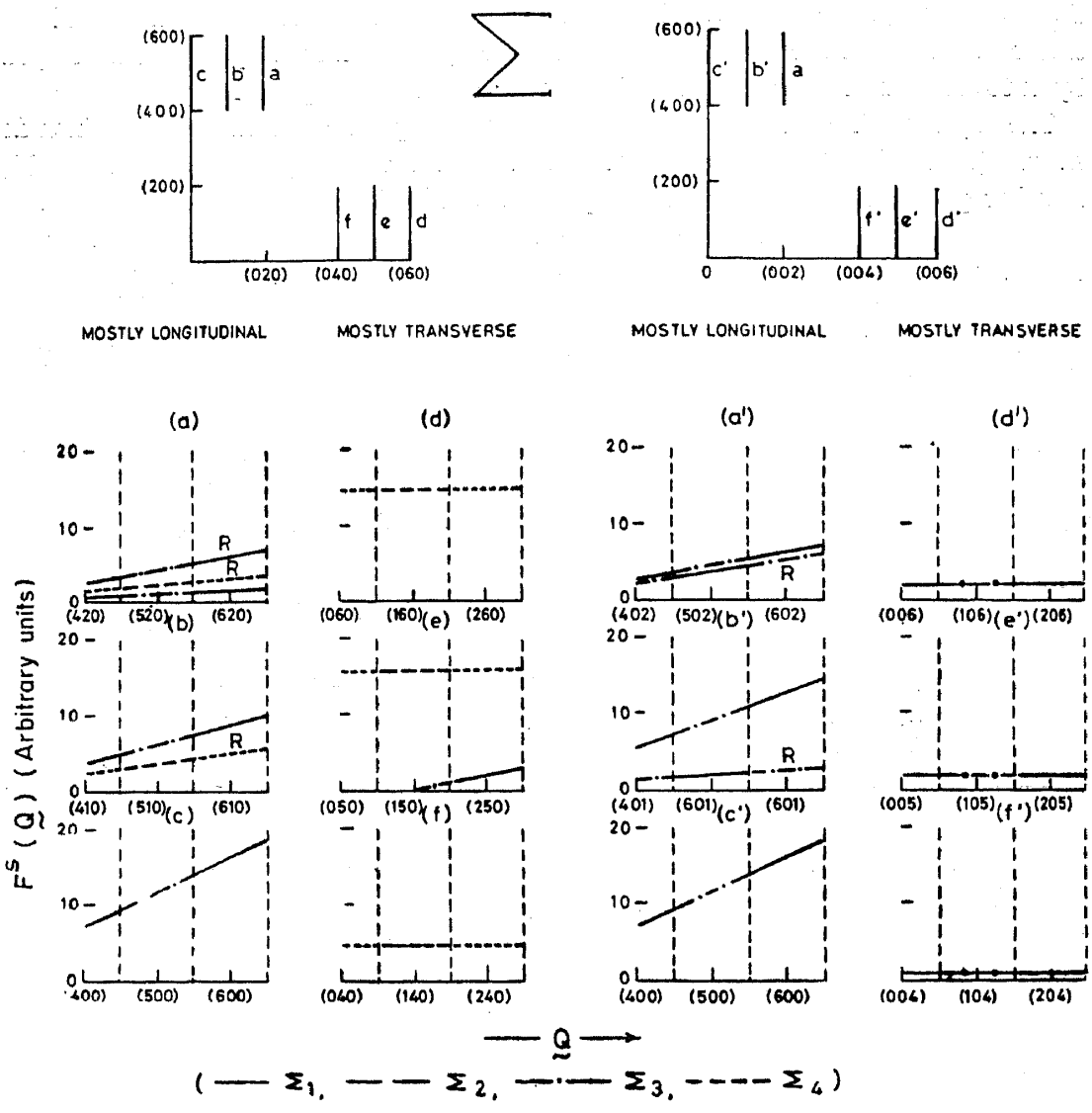

Figure 4 a. Inelastic structure factors for neutron scattering along Σ direction.

Λ_2 modes predominantly contribute to inelastic cross-section compared to Λ_1, Λ_3 and Λ_4 modes. At G=(060), (600) and (601) Λ_3, Λ_4 and Λ_1 modes respectively are to be observed for similar reasons as against other modes. In general, it is observed that translational modes are likely to have larger cross sections compared to the rotational modes. From this kind of considerations, we have chosen suitable regions of reciprocal space for measurement of phonons. In figure 4 we have shown variation of the structure factors along various lines in the reciprocal space for studying Σ, Δ, Λ phonons. Structure factors not shown in this figure are identically zero or negligible compared to the others shown here. Evaluation and use of group theoretical selection rules has helped considerably in favourable choice of reciprocal space for measurements discussed in the next section.

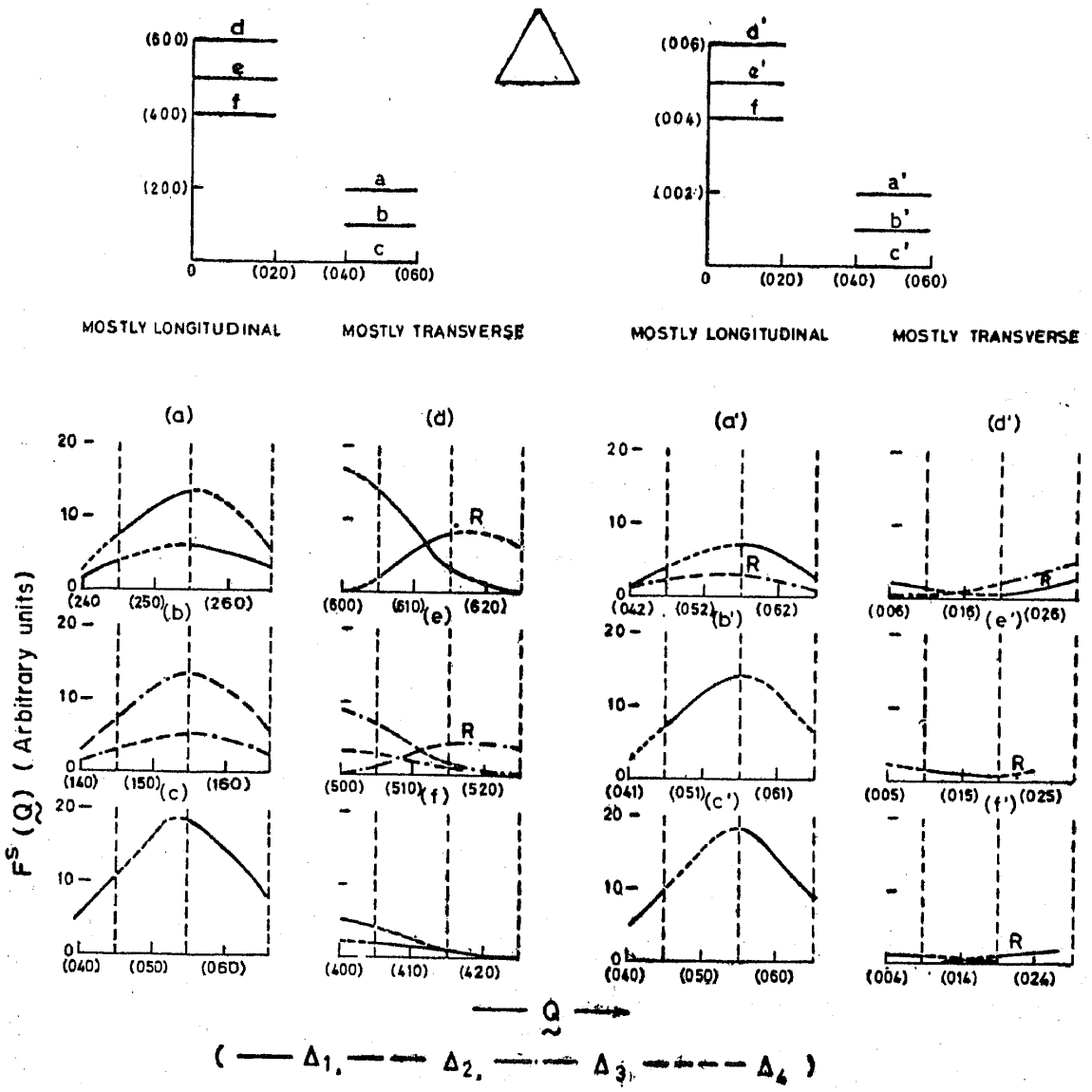

4 b. Inelastic structure factors for neutron scattering along Δ direction.

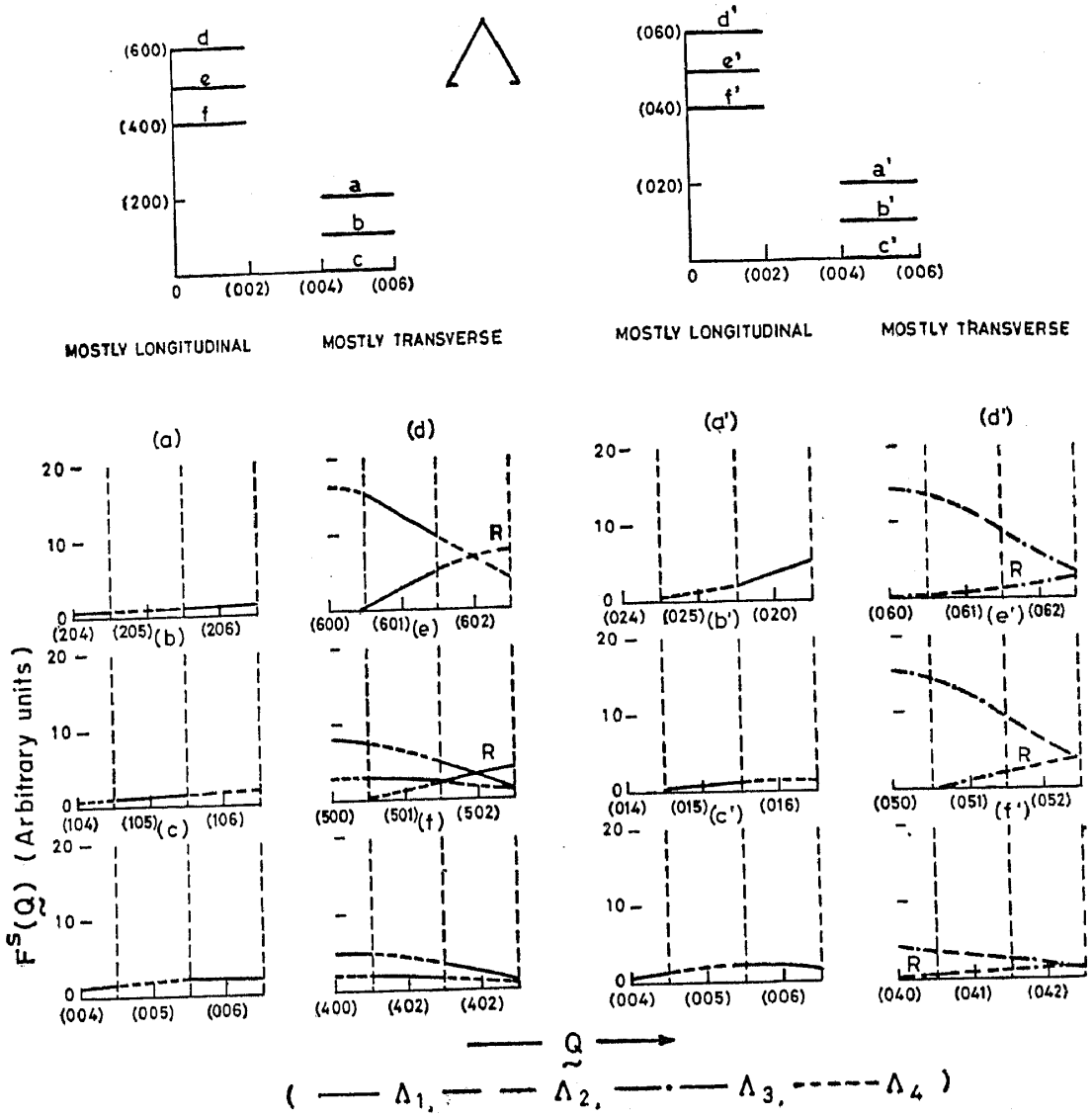

4 c. Inelastic structure for neutron scattering along Λ direction.

5. Experiment

5.1. *Measurements*

We have used a single crystal of KNO_3 (of nearly $4\times3\times3$ cm^3 size) grown by slow evaporation from a saturated aqueous solution held at a temperature of about 45°C. Phonon measurements have been carried out using one of the triple axis spectrometers at CIRUS reactor at Trombay (neutron flux nearly 6×10^{13} cm^{-2} s^{-1}). The incident neutron wavelength (using Cu (111) monochromator) was held at 1·43 Å in most of the measurements. A few measurements were carried out using a wavelength of 1·2Å for purposes of cross-checking. A Cu (111) analyser was used throughout. Constant Q and ϵ techniques (Brockhouse 1960) were employed, and mostly we resorted to neutron energy loss scans. Focusing geometries were resorted to define the phonons as well as one can (Cooper and Nathans 1967; Peckham *et al* 1967). The

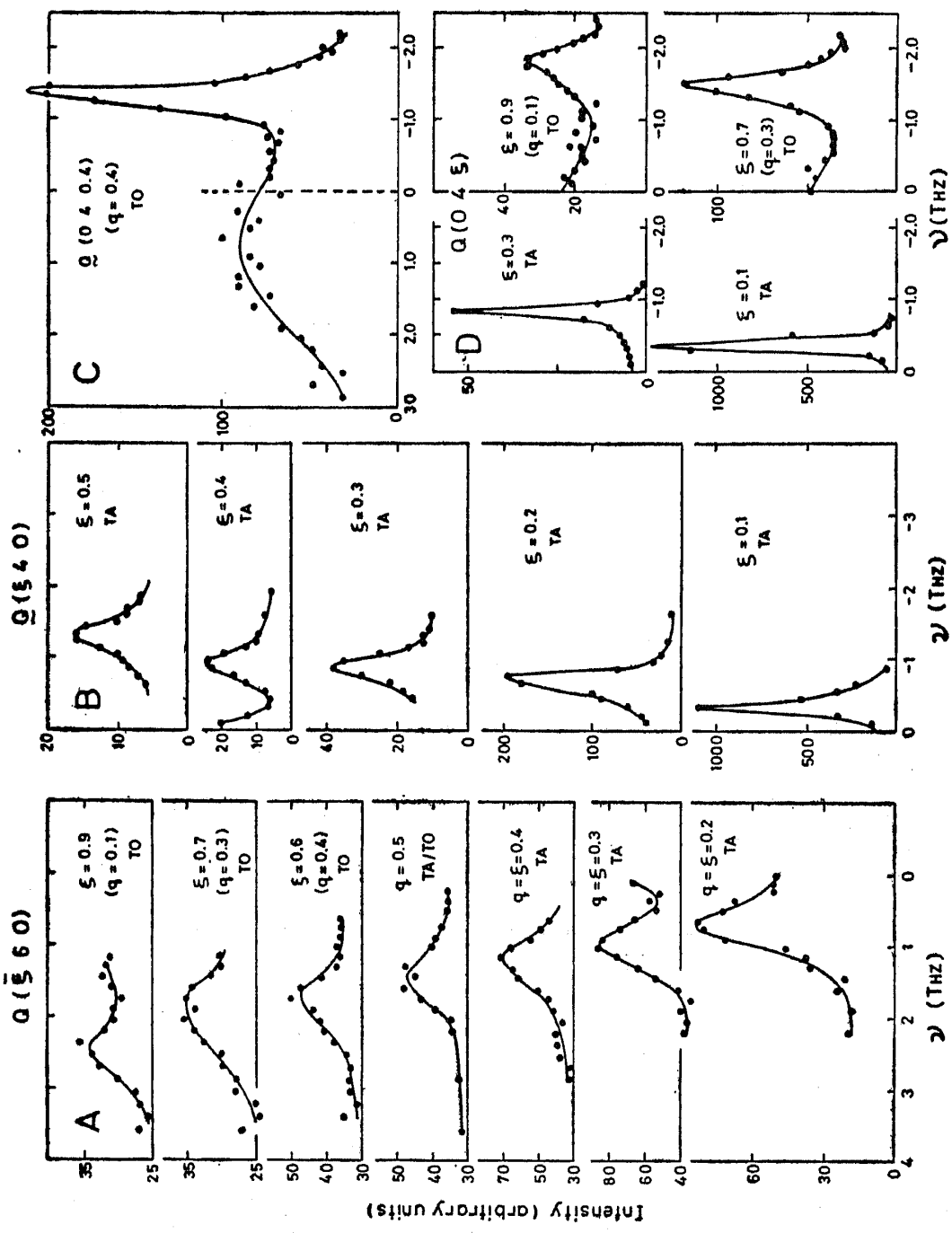

Figure 5. (i) **A.** Transverse phonons along (ξ00) by constant **Q** technique—energy gain process. TA and TO represent the acoustic and optic phonons respectively. **B.** Transverse phonons along (ξ00) by constant **Q** technique—energy loss process. TA and TO represent the acoustic and optic phonons respectively. **C.** Example of a transverse optic phonon observed by energy gain and energy loss processes at a given **Q**. The energy loss group is focussed whereas on the energy gain side the neutron group is defocussed at this wave vector transfer (0 4 0·4). **D.** Typical transverse phonons along (00ξ) by constant **Q** technique—energy loss process.

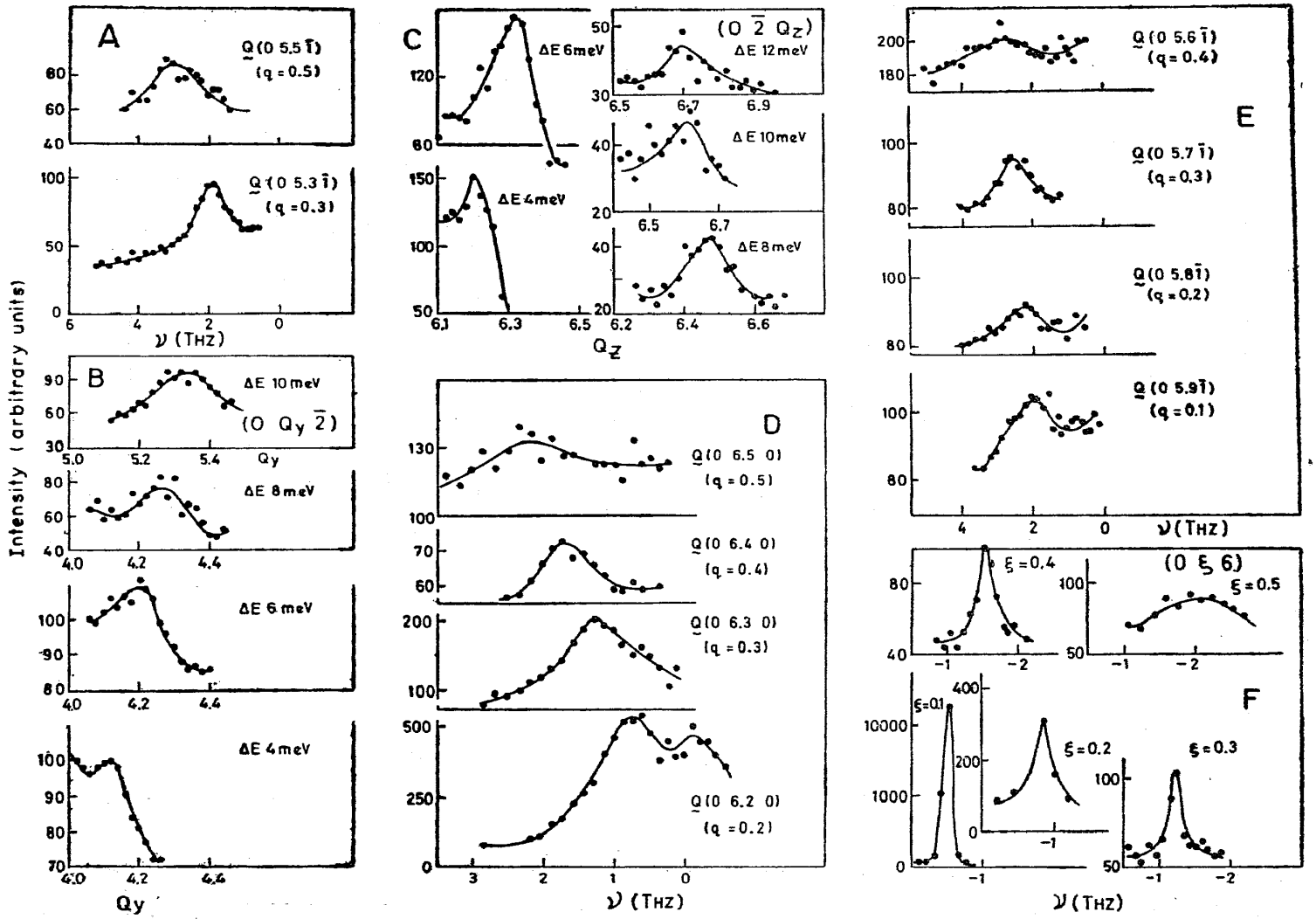

Figure 5. (ii) **A.** Typical longitudinal optic phonons along $(0\xi 0)$ observed by constant **Q** technique—energy gain process. **B.** Longitudinal acoustic phonons along $(0\xi 0)$ observed by constant ϵ technique. **C.** Longitudinal acoustic phonons along (00ξ) observed by constant ϵ technique. **D.** Longitudinal acoustic phonons along $(\xi 00)$ observed by constant **Q** technique—energy gain process. **E.** Longitudinal optic phonons along $(0\xi 0)$ observed by constant **Q** technique—energy gain process. **F.** Transverse phonons along $(0\xi 0)$ observed by constant **Q** technique—energy loss process.

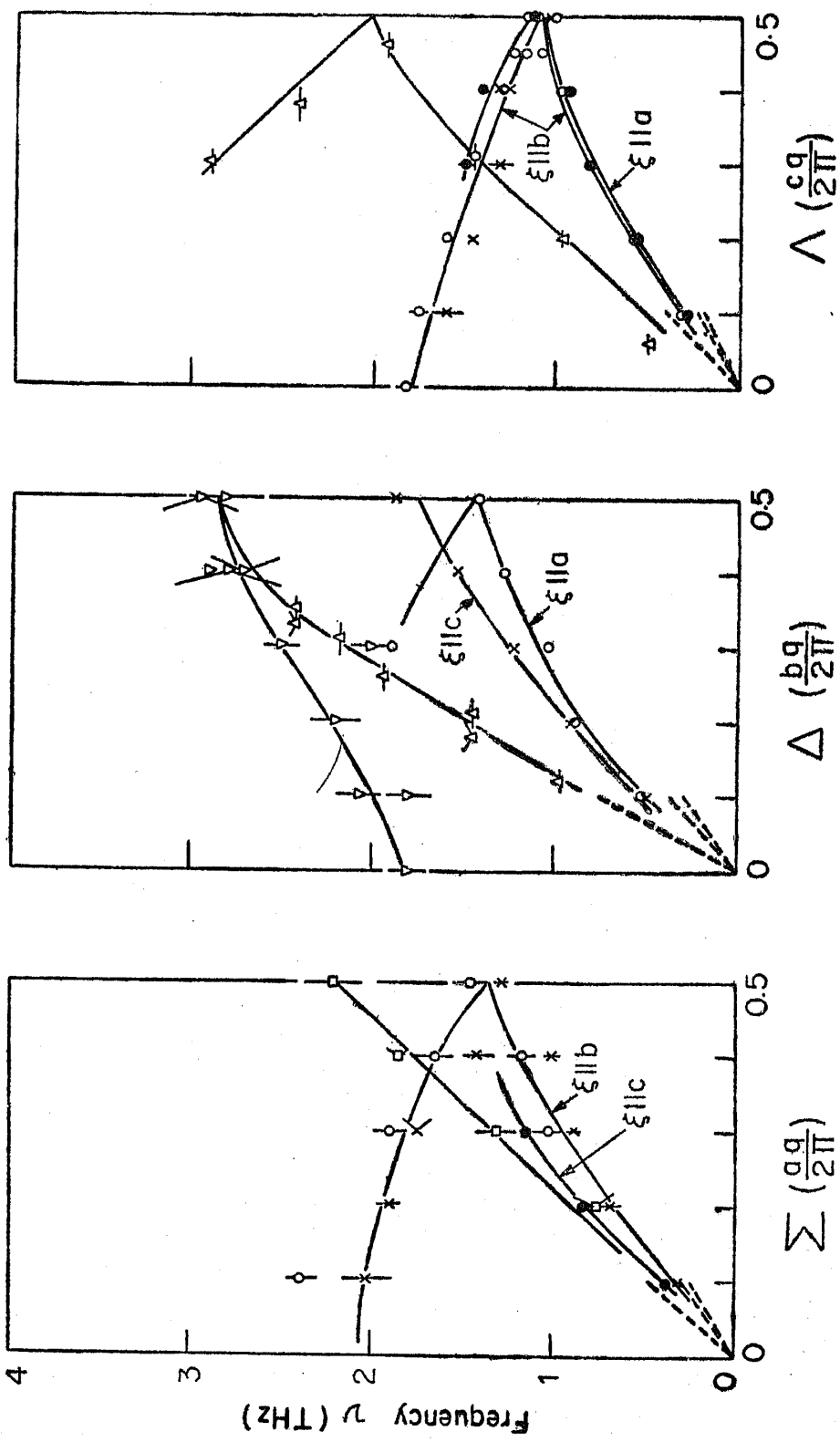

Figure 6. Dispersion curves of phonons along Σ, Δ and Λ directions (uncorrected for resolution effects). Continuous lines are a guide to the eye.

wavelength resolution $\Delta\lambda/\lambda$ is 6% at 1·43 Å as measured by energy analysis of the incoherent elastic peak from vanadium.

The measurements of phonon frequencies were made along the three symmetry directions $\Sigma(\xi, 0, 0)$, $\Delta(0, \xi, 0)$ and $\Lambda(0, 0, \xi)$. Figure 5 shows several experimental line shapes obtained along these directions by constant **Q** and ϵ techniques in energy loss and sometimes in energy gain scans.

Figure 6 shows the dispersion curves obtained by using frequencies corresponding to centre of observed neutron groups (that is frequencies not corrected for resolution effects). Error bars on the frequencies correspond to expected uncertainties taken to be 10% of the full width at half maximum of the neutron groups.

5.2. *Resolution corrections to measured data*

The resolution function of the triple axis neutron spectrometer for inelastic scattering measurements for a nominal setting $(\mathbf{Q}_0, \omega_0)$ of the spectrometer is given by

$$R(\mathbf{Q}-\mathbf{Q}_0, \omega-\omega_0)=R_0(\mathbf{Q}_0, \omega_0) \times\exp\left\{-\frac{1}{2}\sum_{k=1}^{4}\sum_{l=1}^{4} M_{kl}(\mathbf{Q}_0, \omega_0)\, X_k\, X_l\right\}. \tag{6}$$

The matrix elements M_{kl} are functions of incident wave vector $\mathbf{k}_i$, momentum and energy transfers $\hbar\mathbf{Q}_0$, $\hbar\omega_0$ and various collimator parameters and mosaic spreads of the monochromator and analyser crystals. X_k (k=1 to 4) represent the three components of $(\mathbf{Q}-\mathbf{Q}_0)$ and $(\omega-\omega_0)$. Expressions for M_{kl} are given by Cooper and Nathans (1967). The counting rate at the detector is given by,

$$N \propto \phi_0 \int \frac{d^2\sigma}{d\Omega d\epsilon} R(\mathbf{Q}-\mathbf{Q}_0, \omega-\omega_0)\, d^3(\mathbf{Q}-\mathbf{Q}_0)\, d(\omega-\omega_0) \tag{7}$$

where ϕ_0 is the number of neutrons incident on the sample and $d^2\sigma/d\Omega d\epsilon$ is given by (1). One can assume that $|F_j(\mathbf{Q})|^2$ in (1) is not varying fast and that ϕ_0 and efficiency of detector are constants and thereby calculate relative line shapes of phonons of a particular branch. We have developed a computer program (Venkatesh 1978) to evaluate the resolution function using the formalism of Cooper and Nathans (1967) and to get the phonon shapes. The input parameters for the software include the divergencies of the various collimators of the spectrometer, expected phonon frequency and gradient of the dispersion surface. We have estimated the gradient of the acoustic branches on the basis of the elastic constants and assume the dispersion surface to be planar with this gradient. For optic branches we have relied on the measured data itself. Figure 7 shows the comparison of calculated and measured line shapes. One can see that although the calculated line shapes are in good agreement with measured line shapes as far as the widths are concerned, the mean position of neutron groups cannot be taken as the phonon frequencies. The observed line shapes occur at positions shifted from the true phonon frequencies (shown by arrows) by as much as 20% of the lowest frequencies measured. Dispersion curves based on the true frequencies are to be compared with theoretical curves.

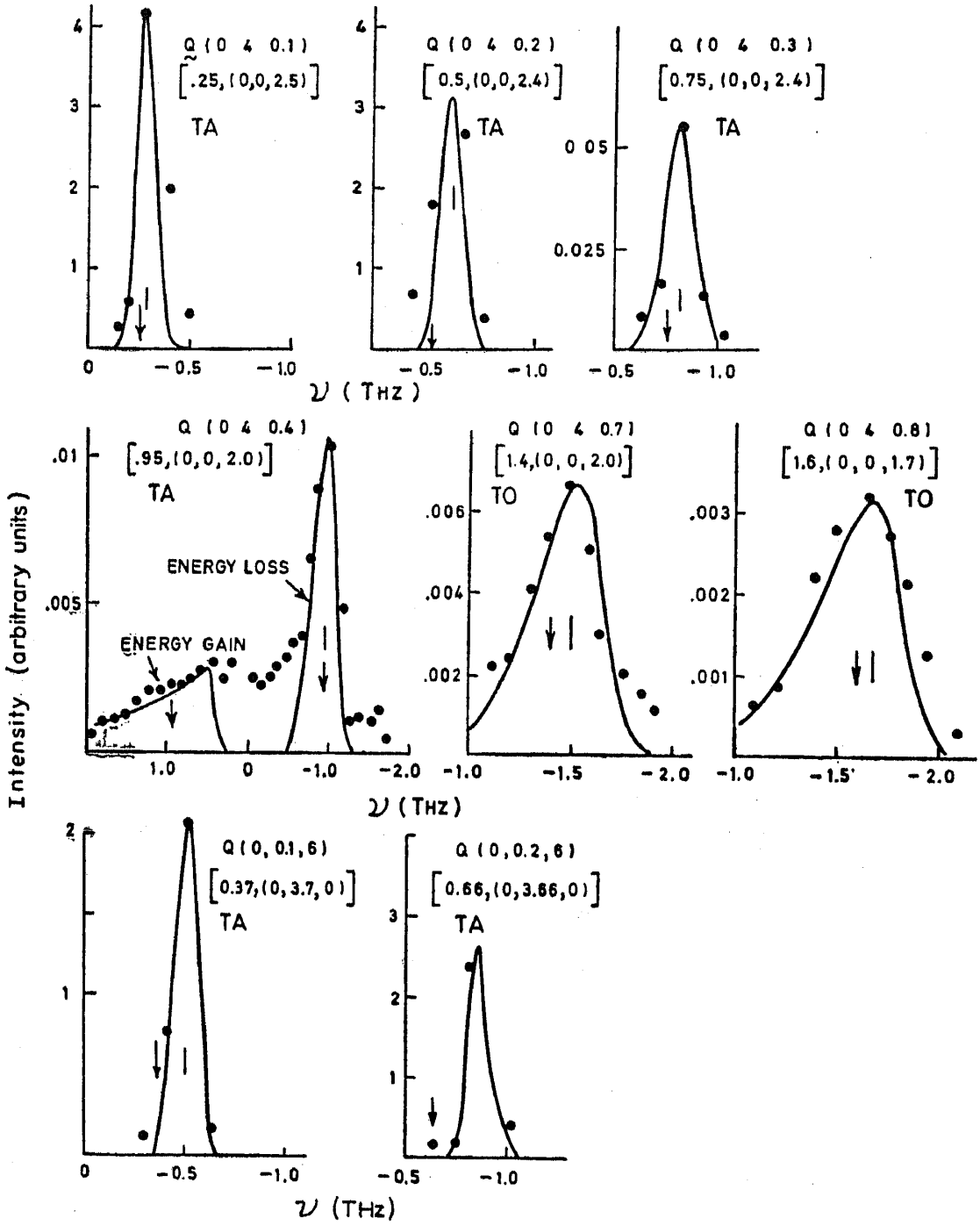

Figure 7. Comparison of numerically evaluated and experimentally measured neutron groups. The numbers in square brackets refer to assumed phonon frequency in THz and cartesian components of the gradient of the dispersion curves in THz Å.

We have seen a series of line shapes indicating observation of spurious phonons. This happened when we were looking for longitudinally polarised phonons along $(0, 2, 6+\xi)$. The frequencies associated with these peaks do not agree with the frequencies expected on the basis of elastic constants for longitudinal acoustic modes and one of the pairs has frequency less than that of transverse acoustic mode also. We believe that one of the peaks is ' spurious ' due to resolution effects and the other occurs at a position shifted considerably from the true longitudinal mode.

6. Theoretical analysis

6.1. *General formulation in the external mode approach*

In the framework of the adiabatic and harmonic approximations (Born and Huang 1954), the crystal potential can be written in terms of the translational and rotational displacements of the atomic and molecular units as follows (Venkataraman and Sahni 1970);

$$\phi = \frac{1}{2} \sum_{\substack{l\kappa\alpha \\ l'\kappa'\beta}} \phi_{\alpha\beta}^{ii'} \begin{pmatrix} l & l' \\ \kappa & \kappa' \end{pmatrix} u_\alpha{}^i \begin{pmatrix} l \\ \kappa \end{pmatrix} u_\beta{}^{i'} \begin{pmatrix} l' \\ \kappa' \end{pmatrix} \tag{8a}$$

with
$$\phi_{\alpha\beta}^{ii'} \begin{pmatrix} l & l' \\ \kappa & \kappa' \end{pmatrix} = \frac{\partial^2 \phi}{\partial u_\alpha{}^i \begin{pmatrix} l \\ \kappa \end{pmatrix} \partial u_\beta{}^{i'} \begin{pmatrix} l' \\ \kappa' \end{pmatrix}}. \tag{8b}$$

Here α and β are the cartesian components x, y and z. $u_\alpha{}^i \begin{pmatrix} l \\ \kappa \end{pmatrix}$ gives displacement of the κ-th unit in the l-th unit cell; when $i=t$ implying translation, $u_\alpha{}^t \begin{pmatrix} l \\ \kappa \end{pmatrix}$ is translational displacement along the α-direction and when $i=r$ implying rotation, $u_\alpha{}^r \begin{pmatrix} l \\ \kappa \end{pmatrix}$ is rotational displacement about the α-axis. l, l' are unit cell indices. κ and κ' denote different atomic or ' molecular ' units in the unit cell.

The equations of motion are given by,

$$m_\kappa \ddot{u}_\alpha{}^t \begin{pmatrix} l \\ \kappa \end{pmatrix} = -\left[\sum_{l'\kappa'\beta} \phi_{\alpha\beta}^{tt} \begin{pmatrix} l & l' \\ \kappa & \kappa' \end{pmatrix} u_\beta^t \begin{pmatrix} l' \\ \kappa' \end{pmatrix} + \sum_{\substack{l'\kappa' \in \mathrm{II} \\ \beta}} \phi_{\alpha\beta}^{tr} \begin{pmatrix} l & l' \\ \kappa & \kappa' \end{pmatrix} u_\beta^r \begin{pmatrix} l' \\ \kappa' \end{pmatrix} \right] \tag{9a}$$

this being the force on $\begin{pmatrix} l \\ \kappa \end{pmatrix}$, and

$$\sum_\beta I_{\alpha\beta}(\kappa) \ddot{u}_\beta^r \begin{pmatrix} l \\ \kappa \end{pmatrix} = -\left[\sum_{l'\kappa'\beta} \phi_{\alpha\beta}^{rt} \begin{pmatrix} l & l' \\ \kappa & \kappa' \end{pmatrix} u_\beta^t \begin{pmatrix} l' \\ \kappa' \end{pmatrix} + \sum_{\substack{l'\kappa' \in \mathrm{II} \\ \beta}} \phi_{\alpha\beta}^{rr} \begin{pmatrix} l & l' \\ \kappa & \kappa' \end{pmatrix} u_\beta^r \begin{pmatrix} l' \\ \kappa' \end{pmatrix} \right] \tag{9b}$$

the torque on $\begin{pmatrix} l \\ \kappa \end{pmatrix}$. The various symbols in these equations have the following meaning: $\kappa \in \mathrm{II}$ implies summation over ' molecular ' units only, m_κ is the mass of the κ-th atomic or ' molecular ' unit; $I_{\alpha\beta}(\kappa)$ denotes the moment of inertia tensor

elements of κ-th ' molecular ' unit. Wave-like solutions of the type

$$U_\alpha{}^i\begin{pmatrix} l \\ \kappa \end{pmatrix} = U_\alpha{}^i\begin{pmatrix} \mathbf{q} \\ \kappa \end{pmatrix} \exp\left[\iota\left\{\mathbf{q}\cdot\mathbf{X}\begin{pmatrix} l \\ \kappa \end{pmatrix} - \omega(\mathbf{q})\, t\right\}\right] \tag{10}$$

($\mathbf{X}\begin{pmatrix} l \\ \kappa \end{pmatrix}$ being the equilibrium position of the κ-th unit in l-th cell with respect to some origin chosen arbitrarily) give rise to $(3\,\mu + 6\nu)$ simultaneous equations in the wave amplitudes $U_\alpha{}^i\begin{pmatrix} \mathbf{q} \\ \kappa \end{pmatrix}$ which can be expressed in matrix notation as

$$\boldsymbol{M}(\mathbf{q})\,\boldsymbol{U}(\mathbf{q}) = \omega^2(\mathbf{q})\,\boldsymbol{m}\,\boldsymbol{U}(\mathbf{q}) \tag{11}$$

where $\boldsymbol{M}(\mathbf{q})$, referred to as the dynamical matrix, has elements given by

$$M_{\alpha\beta}^{ii'}\begin{pmatrix} \mathbf{q} \\ \kappa\kappa' \end{pmatrix} = \sum_{l'} \phi_{\alpha\beta}^{ii'}\begin{pmatrix} 0 & l' \\ \kappa & \kappa' \end{pmatrix} \exp\left[i\,\mathbf{q}\cdot\mathbf{X}\begin{pmatrix} 0 & l' \\ \kappa & \kappa' \end{pmatrix}\right] \tag{12a}$$

and $$m_{\alpha\beta}^{ii'}(\kappa\kappa') = m_\kappa\,\delta_{\alpha\beta}\,\delta_{\kappa\kappa'}\,\delta_{ii'} \quad \text{for } i=t$$

$$= I_{\alpha\beta}(\kappa)\,\delta_{\kappa\kappa'}\,\delta_{ii'} \quad \text{for } i=r$$

with $$m_\kappa = \sum_{k\in\kappa} m_k \tag{12b}$$

and $$I_{\alpha\beta}(\kappa) = \sum_{k\in\kappa} m_k\{|\,\mathbf{X}(k)|^2\,\delta_{\alpha\beta} - \mathbf{X}_\alpha(k)\,\mathbf{X}_\beta(k)\}. \tag{12c}$$

Here k denotes different atoms in a unit and

$$\mathbf{X}\begin{pmatrix} 0 & l' \\ \kappa & \kappa' \end{pmatrix} = \mathbf{X}\begin{pmatrix} l' \\ \kappa' \end{pmatrix} - \mathbf{X}\begin{pmatrix} 0 \\ \kappa \end{pmatrix} \tag{13a}$$

$$\mathbf{X}(k) = \mathbf{X}\begin{pmatrix} 0 \\ \kappa k \end{pmatrix} - \mathbf{X}\begin{pmatrix} 0 \\ \kappa \end{pmatrix}. \tag{13b}$$

The dynamical problem reduces to solving the eigenvalue equation (11), requiring that the wave amplitudes have nontrivial solutions. The eigenvalues $\omega_j{}^2(\mathbf{q})$ $(j=1 \ldots 3\mu+6\nu)$ are obtained by solving the equation,

$$|\,\boldsymbol{M}(\mathbf{q}) - \omega^2(\mathbf{q})\,\boldsymbol{m}\,| = 0. \tag{14}$$

From this discussion, we therefore find that the crux of the problem is to define a suitable crystal potential or a suitable model for the force constants in order to calculate the dynamical matrix.

6.2. *Properties of the force constants and their sum rules*

The force constants defined by (8) have to satisfy certain properties arising from the space group symmetry of the crystal. These properties help in the simplification of the dynamical problem. In addition, the force constants are also required to obey certain sum rules resulting from the fact that an infinitesimal translation or infinitesimal rotation of the crystal as a whole does not produce any restoring force or torque on any vibrating unit. Any potential function or force constant model chosen for the dynamical calculation should therefore satisfy the properties of the force constants and sum rules described below (Venkataraman and Sahni 1970).

(i) Assuming that the potential function ϕ is well behaved,

$$\phi_{\alpha\beta}^{ii'}\begin{pmatrix} l & l' \\ \kappa & \kappa' \end{pmatrix} = \phi_{\beta\alpha}^{i'i}\begin{pmatrix} l' & l \\ \kappa' & \kappa \end{pmatrix}. \tag{15a}$$

(ii) Due to the translational symmetry of the lattice,

$$\phi_{\alpha\beta}^{ii'}\begin{pmatrix} l & l' \\ \kappa & \kappa' \end{pmatrix} = \phi_{\alpha\beta}^{ii'}\begin{pmatrix} l+L & l'+L \\ \kappa & \kappa' \end{pmatrix}. \tag{15b}$$

(iii) Let

$$S_m = \{S/\mathrm{v}(S) + \mathbf{X}(m)\},$$

a space group operation, acting on the undistorted crystal produce the transformations

$$\mathbf{X}\begin{pmatrix} l \\ \kappa \end{pmatrix} \xrightarrow{S_m} \mathbf{X}\begin{pmatrix} L \\ K \end{pmatrix} \text{ and } \mathbf{X}\begin{pmatrix} l' \\ \kappa' \end{pmatrix} \xrightarrow{S_m} \mathbf{X}\begin{pmatrix} L' \\ K' \end{pmatrix}.$$

Then,

$$\boldsymbol{\phi}^{ii'}\begin{pmatrix} L & L' \\ K & K' \end{pmatrix} = c^i(S)\, \boldsymbol{S}\, \boldsymbol{\phi}^{ii'}\begin{pmatrix} l & l' \\ \kappa & \kappa' \end{pmatrix} \widetilde{\boldsymbol{S}}\; c^{i'}(s). \tag{15c}$$

where

$$c^i(S) = 1 \qquad \text{for } i = t,$$

$$= |\boldsymbol{S}| \qquad \text{for } i = r.$$

(iv) Since an infinitesimal translation produces no restoring force or torque on any vibrating unit,

$$\sum_{l'\kappa'} \phi_{\alpha\beta}^{tt}\begin{pmatrix} o & l' \\ \kappa & \kappa' \end{pmatrix} = 0, \tag{15d}$$

and

$$\sum_{l'\kappa'} \phi_{\alpha\beta}^{rt}\begin{pmatrix} o & l' \\ \kappa & \kappa' \end{pmatrix} = 0. \tag{15e}$$

(v) Again, since an infinitesimal rotation does not produce any restoring force or torque on any vibrating unit,

$$\sum_{l'\kappa'}{}' \sum_{\gamma\delta} \epsilon_{\beta\gamma\delta} X_\gamma \begin{pmatrix} o & l' \\ \kappa & \kappa' \end{pmatrix} \phi^{tt}_{\alpha\delta} \begin{pmatrix} o & l' \\ \kappa & \kappa' \end{pmatrix} + \sum_{l'\kappa' \in II} \phi^{tr}_{\alpha\beta} \begin{pmatrix} o & l' \\ \kappa & \kappa' \end{pmatrix} = 0, \quad (15f)$$

and

$$\sum_{l'\kappa'}{}' \sum_{\gamma\delta} \epsilon_{\beta\gamma\delta} X_\gamma \begin{pmatrix} o & l' \\ \kappa & \kappa' \end{pmatrix} \phi^{rt}_{\alpha\delta} \begin{pmatrix} o & l' \\ \kappa & \kappa' \end{pmatrix} + \sum_{l'\kappa' \in II} \phi^{rr}_{\alpha\beta} \begin{pmatrix} o & l' \\ \kappa & \kappa' \end{pmatrix} = 0. \quad (15g)$$

6.3. *Constraints on the force constants and hermiticity of the dynamical matrix*

The sum rules described in § 6.2 eqs (15d) to (15g) are useful in determination of the self-terms $\phi^{ii'}_{\alpha\beta} \begin{pmatrix} o & o \\ \kappa & \kappa \end{pmatrix}$. We have

$$\phi^{tt}_{\alpha\beta} \begin{pmatrix} o & o \\ \kappa & \kappa \end{pmatrix} = -\sum_{l'\kappa'}{}' \phi^{tt}_{\alpha\beta} \begin{pmatrix} o & l' \\ \kappa & \kappa' \end{pmatrix}, \quad (16a)$$

$$\phi^{rt}_{\alpha\beta} \begin{pmatrix} o & o \\ \kappa & \kappa \end{pmatrix} = -\sum_{l'\kappa'}{}' \phi^{rt}_{\alpha\beta} \begin{pmatrix} o & l' \\ \kappa & \kappa' \end{pmatrix}, \quad (16b)$$

$$\phi^{tr}_{\alpha\beta} \begin{pmatrix} o & o \\ \kappa & \kappa \end{pmatrix} = -\sum_{l'\kappa' \in II}{}' \phi^{tr}_{\alpha\beta} \begin{pmatrix} o & l' \\ \kappa & \kappa' \end{pmatrix} - \sum_{l'\kappa'}{}' \sum_{\gamma\delta} \epsilon_{\beta\gamma\delta} X_\gamma \begin{pmatrix} o & l' \\ \kappa & \kappa' \end{pmatrix} \phi^{tt}_{\alpha\delta} \begin{pmatrix} o & l' \\ \kappa & \kappa' \end{pmatrix}, \quad (16c)$$

$$\phi^{rr}_{\alpha\beta} \begin{pmatrix} o & o \\ \kappa & \kappa \end{pmatrix} = -\sum_{l'\kappa' \in II}{}' \phi^{rr}_{\alpha\beta} \begin{pmatrix} o & l' \\ \kappa & \kappa' \end{pmatrix} - \sum_{l'\kappa'}{}' \sum_{\gamma\delta} \epsilon_{\beta\gamma\delta} X_\gamma \begin{pmatrix} o & l' \\ \kappa & \kappa' \end{pmatrix} \phi^{rt}_{\alpha\delta} \begin{pmatrix} o & l' \\ \kappa & \kappa' \end{pmatrix}, \quad (16d)$$

where prime over summation indicates omission of term $\begin{pmatrix} l' \\ \kappa' \end{pmatrix}$ equal to $\begin{pmatrix} o \\ \kappa \end{pmatrix}$.

These equations (16a–16d) combined with the equation

$$\phi^{ii'}_{\alpha\beta} \begin{pmatrix} o & o \\ \kappa & \kappa \end{pmatrix} = \phi^{i'i}_{\beta\alpha} \begin{pmatrix} o & o \\ \kappa & \kappa \end{pmatrix}, \quad (16e)$$

result in several constraints on the force constants, for example,

$$\sum_{l'\kappa'}{}' \phi^{tt}_{\alpha\beta} \begin{pmatrix} o & l' \\ \kappa & \kappa' \end{pmatrix} = \sum_{l'\kappa'}{}' \phi^{tt}_{\beta\alpha} \begin{pmatrix} o & l' \\ \kappa & \kappa' \end{pmatrix}. \quad (16f)$$

Any dynamical model should satisfy these constraints, otherwise the dynamical matrix as calculated using (16a) to (16d) will not be hermitean. If the force constants are treated as parameters or obtained from a potential function, these constraints may be imposed on the parameters or on the potential function. In particular, if a two body potential function

$$\phi = \tfrac{1}{2} \sum_{\substack{l\kappa\, l'\kappa' \\ k\in\kappa \\ k'\in\kappa'}}{}' V_{\kappa k,\,\kappa' k'} \left\{ \left| r \begin{pmatrix} l & l' \\ \kappa k & \kappa' k' \end{pmatrix} \right| \right\}. \tag{17}$$

is used, the translational sum rules are automatically satisfied.

Here, $\mathbf{r}\begin{pmatrix} l & l' \\ \kappa k & \kappa' k' \end{pmatrix} = \mathbf{r}\begin{pmatrix} l' \\ \kappa' k' \end{pmatrix} - \mathbf{r}\begin{pmatrix} l \\ \kappa k \end{pmatrix}$ and

$\mathbf{r}\begin{pmatrix} l \\ \kappa k \end{pmatrix}$ denotes instantaneous position of $\begin{pmatrix} l \\ \kappa k \end{pmatrix}$.

It can be shown that the rotational sum rules are also satisfied, if

$$\left.\frac{\partial \phi}{\partial r_\alpha \begin{pmatrix} o \\ \kappa k \end{pmatrix}}\right|_0 = 0 \quad \text{for all } \kappa,\ k \in \kappa \text{ and } \alpha. \tag{18a}$$

We define

$$-\frac{\partial \phi}{\partial r_\alpha \begin{pmatrix} o \\ k\kappa \end{pmatrix}} = -\frac{\partial}{\partial r_\alpha \begin{pmatrix} o \\ \kappa k \end{pmatrix}} \left[\sum_{\substack{l'\kappa' \\ k'\in\kappa'}}{}' V_{\kappa k,\,\kappa' k'} \left\{ \left| r \begin{pmatrix} o & l' \\ \kappa k & \kappa' k' \end{pmatrix} \right| \right\} \right] \tag{18b}$$

as 'external force' on atom at $\begin{pmatrix} o \\ \kappa k \end{pmatrix}$ in the α-direction. Thus the constraint (18a) means that the external force on different atoms in their equilibrium positions be zero. If this constraint is not satisfied, it may result in the lattice being unstable and the eigenvalues $\omega_j^2(\mathbf{q})$ of the dynamical matrix may come out to the negative. We shall come back to this point in § 7.2.

6.4. *Properties of the dynamical matrix, group theoretical simplification of the dynamical problem and symmetry classification of normal modes*

Just as the force constants have to satisfy certain general properties as mentioned in § 6.2, the dynamical matrix (elements) satisfies the following relations due to space group symmetry, we list these properties in addition to other group theoretical aspects (Venkataraman and Sahni 1970)

(i) $\boldsymbol{M}(\mathbf{q}) = \boldsymbol{M}^+(\mathbf{q})$ (19a)

(ii) $\boldsymbol{M}(\mathbf{q}) = \boldsymbol{M}^*(-\mathbf{q})$, (19b)

(iii) $\boldsymbol{M}(\mathbf{q}+\mathbf{G}) = \boldsymbol{u}\,\boldsymbol{M}(\mathbf{q})\,\boldsymbol{u}^+$ (19c)

where **G** is any reciprocal lattice vector, and $\boldsymbol{u}$ is a unitary diagonal matrix consisting of elements

$$u^{ii'}_{\alpha\beta}(\kappa\,\kappa') = \delta_{\alpha\beta}\,\delta_{\kappa\kappa'}\,\delta_{ii'}\exp\{-i\mathbf{G}\cdot\mathbf{X}(\kappa)\}. \tag{19d}$$

(iv) If $S_m = \{S \mid \mathbf{v}(S) + \mathbf{X}(m)\} \in G$, the space group of the crystal, then

$$\Gamma(\mathbf{q}, S_m)\,\boldsymbol{M}(\mathbf{q})\,\Gamma^{+}(\mathbf{q}, S_m) = \boldsymbol{M}(S\mathbf{q}). \tag{19e}$$

The matrix $\Gamma(\mathbf{q}, S_m)$ consists of elements

$$\Gamma^{ii'}_{\alpha\beta}(\kappa\kappa' \mid \mathbf{q}, S_m) = c^{i}(S)\,\delta_{ii'}\,S_{\alpha\beta}\,\delta(\kappa, F_0(\kappa', S))$$

$$\times \exp[-i(S\mathbf{q})\cdot(\mathbf{v}(S) + \mathbf{X}(m))], \tag{19f}$$

where $\delta(\kappa, F_0(\kappa', S)) = 1$ when $\kappa = F_0(\kappa', S)$

$$= 0 \text{ otherwise} \tag{19g}$$

with $F_0(\kappa', S)$ being the sublattice arrived at from the sublattice κ' via S_m.

(v) If $\boldsymbol{R} \in G_0(\mathbf{q})$, the point group of $\mathbf{q}$, ($\boldsymbol{R}\mathbf{q} = \mathbf{q} + \mathbf{G}$) then since $\boldsymbol{M}(\boldsymbol{R}\mathbf{q}) = \boldsymbol{M}(\mathbf{q} + \mathbf{G}) = \boldsymbol{u}\,\boldsymbol{M}(\mathbf{q})\,\boldsymbol{u}^{+}$, we have by using (19e)

$$\boldsymbol{T}(\mathbf{q}, R)\,\boldsymbol{M}(\mathbf{q})\,\boldsymbol{T}^{+}(\mathbf{q}, R) = \boldsymbol{M}(\mathbf{q}), \tag{19h}$$

where $\boldsymbol{T}(q, R) = \boldsymbol{u}^{+}\,\Gamma(q, R_m)\exp[i\,\mathbf{q}\cdot\{\mathbf{v}(R) + \mathbf{X}(m)\}]$.

The matrix $\mathbf{T}(\mathbf{q}, R)$ consists of elements*

$$T^{ii'}_{\alpha\beta}(\kappa\kappa' \mid \mathbf{q}, R) = \delta_{ii'}\,c^{i}(R)\,R_{\alpha\beta}\,\delta(\kappa, F_0(\kappa', R))$$

$$\times \exp[i\,\mathbf{G}\cdot\{\mathbf{X}(\kappa) - \mathbf{v}(R)\}] \tag{19i}$$

(vi) If $\boldsymbol{S}_{-} \in G_0$, the point group of the crystal, such that

$$\boldsymbol{S}_{-}\,\mathbf{q} = -\mathbf{q} + \mathbf{G},$$

then, since $\boldsymbol{M}(\boldsymbol{S}_{-}\mathbf{q}) = \boldsymbol{M}(-\mathbf{q} + \mathbf{G}) = \boldsymbol{u}\,\boldsymbol{M}(-\mathbf{q})\,\boldsymbol{u}^{+} = \boldsymbol{u}\,\boldsymbol{M}^{*}(\mathbf{q})\,\boldsymbol{u}^{+}$, we have by using (19e)

$$\Gamma(\mathbf{q}, S_{-m})\,\boldsymbol{M}(\mathbf{q})\,\Gamma^{+}(\mathbf{q}, S_{-m}) = \boldsymbol{u}\,\boldsymbol{M}^{*}(\mathbf{q})\,\boldsymbol{u}^{+},$$

or $$\boldsymbol{T}(\mathbf{q}, S_{-})\,\boldsymbol{M}(\mathbf{q})\,T^{+}(\mathbf{q}, S_{-}) = \boldsymbol{M}^{*}(\mathbf{q}). \tag{19j}$$

Here $$\boldsymbol{T}(\mathbf{q}, S_{-}) = \boldsymbol{u}^{+}\,\Gamma(\mathbf{q}, S_{-m})\exp[-i\,\mathbf{q}\cdot\{\mathbf{v}(S_{-}) + \mathbf{X}(m)\}].$$

*Our $T^{ii'}_{\alpha\beta}(\kappa\kappa' \mid \mathbf{q}, R)$ differs from that given by Venkataraman and Sahni (1970). This is because our dynamical matrix contains an additional phase term.

Elements of $\boldsymbol{T}$ (q, S_-) are given by (19i) with R replaced by S_-.

Relations (19h) to (19j) are useful in finding out relations between different elements of the dynamical matrix. In this way one can recognise the independent elements of the dynamical matrix and thereby reduce evaluation of the large number of dynamical matrix elements to that of a few independent ones.

The matrices $\boldsymbol{T}$ (q, R) are unitary. The set of matrices $\{\boldsymbol{T}$ (q, R) $\mid \boldsymbol{R} \in G_0$ (q)$\}$ form a reducible multiplier representation of G_0 (q).

According to standard group theoretical arguments, the number of times a given sth irreducible multiplier representation (IMR) appears in the matrix T is given by

$$C_s = \frac{1}{h} \sum_R \chi [\boldsymbol{T} (\mathbf{q}, R)] \chi^* [\tau^s (\mathbf{q}, R)], \tag{20}$$

where h is the order of the group G_0 (q), τ^s (q, R) is the sth IMR corresponding to the point group operation R in G_0 (q), $\chi [\boldsymbol{T}$ (q, R)] and $\chi [\tau^s$ (q, R)] are respectively characters of the $\boldsymbol{T}$(q, R) and τ^s (q, R) matrices. Kovalev (1964) has given tables of IMRs for lattices having different space groups and corresponding to various wavevectors.

Symmetry vectors belonging to various representations (IMRs) can be used for block-diagonalising the dynamical matrix. This helps to classify the eigenvalues representation by representation. The symmetry vectors can be determined from the projection operators,

$$P_{ij}^s (\mathbf{q}) = \frac{f_s}{h} \sum_R \tau_{ij}^{s*} (\mathbf{q}, R) \boldsymbol{T} (\mathbf{q}, R), \tag{21}$$

where f_s is the dimensionality of the IMR τ^s. These vectors are used in block diagonalising the dynamical matrix using the relation

$$\mathscr{M} (\mathbf{q}) = \boldsymbol{\xi}^\dagger (\mathbf{q}) \boldsymbol{M} (\mathbf{q}) \boldsymbol{\xi} (\mathbf{q}), \tag{22}$$

where $\mathscr{M}$ (q) is the block-diagonalised dynamical matrix and $\boldsymbol{\xi}$ (q) is the symmetry vector matrix. Details of this method are described by Venkataraman and Sahni (1970) and Maradudin and Vosko (1968).

The various blocks of the block-diagonalised dynamical matrix belong to different IMRs. The size of the blocks is given by (20); the order of the block is equal to the number of times the representation occurs in the T matix. The phonon frequencies obtained by diagonalising these blocks are said to belong to the corresponding representation and hence labelling is achieved.

7. Dynamical model calculation in the external mode approach

7.1. *Rigid molecular-ion model*

In the last section we described a general formulation of the dynamical problem in the external mode approach. We also discussed certain constraints which have to

be satisfied by the dynamical model. In this section, we describe a dynamical model which may be applied to ionic or partly ionic crystals containing ' molecular ' units.

The rigid-ion model is well known in lattice dynamics. Here one considers the constituents of an ionic lattice as ' atomic ' rigid units and does not take into account relative displacements between the atomic core and outer electronic shells and therefore does not consider polarisabilities of the ions. In the external mode approach where certain 'molecular' units are considered rigid, one can still work out the dynamics in the spirit of rigid-ion model. To differentiate the situation from the conventional rigid-ion model we refer to this as rigid molecular-ion model. In this model, one assumes some effective ionic charges to be situated at the positions of atoms constituting the ' molecules '. These charges interact via the long range Coulombic interaction with all other charges in the lattice. The effective ionic charges may be treated as parameters in the model. One also assumes that short range forces act between the atomic units and atoms constituting the 'molecules'. Different kinds of interaction may be assumed for this purpose. We assume Born-Mayer type short range potential. Thus the crystal potential* ϕ consists of two body potentials between atoms of different molecular units given by

$$V(r_{12}) = \frac{1}{4\pi\epsilon_0}\,\frac{Z_1 Z_2 e^2}{r_{12}} + a \exp\left\{\frac{-13{\cdot}6\, r_{12}}{1{\cdot}1\,(R_1+R_2)}\right\}. \tag{23}$$

Here Z_1 and Z_2 are ' effective charges ' situated at the centre of masses of the interacting atoms. R_1 and R_2 may be called the ' effective radii ' of atoms. ϵ_0 is the permittivity constant, $1/4\pi\epsilon_0 = 9{\cdot}0 \times 10^9\ nt - m^2/\text{coul}^2$. Following Kitaigorodsky and Mirskaya (1964), we choose $a = 4{\cdot}2 \times 10^4$ kcal/mole$=1822{\cdot}0$ ev/atom. The effective charges and radii are treated as parameters of the model.

7.2. *Constraints on the potential function*

We have mentioned in §6·3 that the constraint on the crystal potential which is made up of two body potentials is

$$\left.\frac{\partial\phi}{\partial r_\alpha\begin{pmatrix}0\\ \kappa k\end{pmatrix}}\right|_0 = 0.$$

Expressing ϕ as sum of two parts, namely ϕ^{C} the Coulombic and ϕ^{SR} the short range parts, we have

$$\phi = \phi^{\mathrm{C}} + \phi^{\mathrm{SR}}. \tag{24}$$

Therefore,

$$\left.\frac{\partial\phi^{\mathrm{C}}}{\partial r_\alpha\begin{pmatrix}0\\ \kappa k\end{pmatrix}}\right|_0 + \left.\frac{\partial\phi^{\mathrm{SR}}}{\partial r_\alpha\begin{pmatrix}0\\ \kappa k\end{pmatrix}}\right|_0 = 0, \tag{25}$$

* Since we are interested only in external modes, force constants are derived by differentiating the crystal potential with respect to only those coordinates which are allowed to vary, namely translations of atoms and 'molecules' and rotation of 'molecules'. Internal coordinates are not allowed to vary. Hence we are dealing with only *external* forces which are obtained by differentiating the potential in which interactions involving atoms on *different* 'molecules' only are involved.

The first term may be obtained by differentiating the Madelung energy of the crystal with respect to $r_\alpha\begin{pmatrix}0\\ \kappa k\end{pmatrix}$ and subtracting from this the contribution due to other atoms in the same molecule. We have

$$\phi^{C} = \frac{1}{2}\sum_{\substack{l\kappa,\, l'\kappa' \\ k\in\kappa \\ k'\in\kappa'}}{}' \frac{1}{4\pi\epsilon_0}\frac{Z_{\kappa k} Z_{\kappa' k'} e^2}{\left|\mathbf{r}\begin{pmatrix} l & l' \\ \kappa k & \kappa' k'\end{pmatrix}\right|}. \tag{26}$$

Thus

$$\left.\frac{\partial \phi^{C}}{\partial r_\alpha\begin{pmatrix}0\\ \kappa k\end{pmatrix}}\right|_0 = \text{Derivative of the Madelung energy} - \sum_{\substack{k'\in\kappa \\ k'\neq k}} \frac{1}{4\pi\epsilon_0}\frac{Z_{\kappa k} Z_{\kappa' k'} X_\alpha\begin{pmatrix} o & o \\ \kappa k & \kappa k'\end{pmatrix}}{\left|\mathbf{X}\begin{pmatrix}0 & 0\\ \kappa k & \kappa' k'\end{pmatrix}\right|^3} \tag{27}$$

Similarly

$$\phi^{SR} = \frac{1}{2}\sum_{\substack{l\kappa,\, l'\kappa' \\ k\in\kappa \\ k'\in\kappa'}}{}' a \exp\left\{\frac{-13{\cdot}6\left|\mathbf{r}\begin{pmatrix} l & l' \\ \kappa k & \kappa' k'\end{pmatrix}\right|}{1{\cdot}1\,(R_{\kappa k} + R_{\kappa' k'})}\right\} \tag{28}$$

and

$$\left.\frac{\partial \phi^{SR}}{\partial r_\alpha\begin{pmatrix}0\\ \kappa k\end{pmatrix}}\right| = \sum_{\substack{l'o' \\ k'\in\kappa'}}{}' \frac{13{\cdot}6\, a}{1{\cdot}1\,(R_{\kappa k} + R_{\kappa' k})}\frac{X_\alpha\begin{pmatrix} o & l' \\ \kappa k & \kappa' k'\end{pmatrix}}{\left|\mathbf{X}\begin{pmatrix}0 & l'\\ \kappa k & \kappa' k'\end{pmatrix}\right|}$$

$$\times \exp\left[\frac{-13{\cdot}6\left|\mathbf{X}\begin{pmatrix} o & l' \\ \kappa k & \kappa' k'\end{pmatrix}\right|}{1{\cdot}1\,(R_{\kappa k} + R_{\kappa' k'})}\right]. \tag{29}$$

We also have the condition of charge neutrality of the unit cell:

$$\sum_{\kappa k} Z_{\kappa k} = 0. \tag{30}$$

In general, the constraint given by (25) may not be satisfied for a given crystal structure. In such a case, the constraints may be applied on the effective charges and radii parameters so as to preserve the structure. A proper set of parameters may be obtained by balancing the Coulombic and short range external forces on different atoms. It may not be necessary to be able to exactly balance the Coulombic and short range forces but considerations like getting real phonon frequencies may be more important in arriving at the parameters, this set of parameters being not necessarily unique. Another consideration that has to be kept in view is that the cohesive energy of the crystal should be of the right order of magnitude. Otherwise one may be fictitiously reducing all the parameters to reduce the forces, but that would be

unphysical. If necessary, the coefficient a in the short range potential may also be treated as a disposable parameter.

Once a proper set of parameters is obtained, the dynamical calculations may be carried through using the formalism in § 6·1. As the crystal potential is made up of two parts ϕ^{C} and ϕ^{SR}, correspondingly the dynamical matrix would also have two parts $\boldsymbol{M}^{C}$ and $\boldsymbol{M}^{SR}$. These two parts may be calculated using the method described in the next two sections. Then the dynamical matrix may be block diagonalised using the group theoretical method outlined in § 6·4. Finally the blocks are diagonalised by brute-force to get the eigenvalues $\omega_j^2(\mathbf{q})$. We have developed a computer program to evaluate $\boldsymbol{M}^{C}$, $\boldsymbol{M}^{SR}$ and the eigenvalues $\omega_j^2(\mathbf{q})$ using the model described in this paper (Chaplot 1978).

7.3. *Electrostatic part of the dynamical matrix*

Because of the long range nature of the Coulombic potential, the summations involved in the evaluation of the dynamical matrix elements pose difficulties. Venkataraman and Sahni (1970) have adopted the methods developed by Ewald (1917) and Kellermann (1940) to obtain analytical expressions for dynamical matrix elements $M_{\alpha\beta}^{c,ii'}\begin{pmatrix}\mathbf{q}\\ \kappa\kappa'\end{pmatrix}$. These expressions involve summations of fast converging series in direct and reciprocal spaces. To the best of our knowledge, these expressions have not been used in lattice dynamical calculations so far.

7.4 *Short range part of the dynamical matrix*

We outline here two different approaches which we have tried.

Model (i)

This model makes use of the so-called 'extended point mass approximation' developed by Rafizadeh and Yip (1970), wherein one assumes that the short range potential can be expressed as a function of the 'net-displacement' of molecules rather than in terms of translations and rotations. Using this assumption the force constants ϕ^{tr}, ϕ^{rt} and ϕ^{rr} are expressed in terms of ϕ^{tt} only (and that was the attraction to try this model) and parameters called the 'effective size' of the molecules. These parameters also depend on the particular pair of molecules between which the interactions are considered. In certain calculations, it was found that taking the effective size parameter

$$\mathbf{R}\begin{pmatrix}l'\\ \kappa'\end{pmatrix} = -\frac{1}{2}\,\mathbf{X}\begin{pmatrix}l & l'\\ \kappa & \kappa'\end{pmatrix} \tag{31}$$

gave quite satisfactory results. If relation (31) is assumed then only ϕ^{tt} have to be obtained through the short range potential of the type (28). Another alternative is to treat ϕ^{tt} as disposable parameters in the dynamical calculation. However, these parameters have to satisfy the constraints given in § 6.3. The self terms have to be

obtained by using the appropriate sum rules. It is not clear to us whether the potential (28) and the corresponding constraints on that potential are compatible with the approximation of extended point mass and with the assumption of expressing the short range potential as a function of net displacement.

Model (ii)

In this model, we make use of the following equations in which the external mode force constants are expressed in terms of the atom-atom force constants (Venkataraman and Sahni 1970)

$$\phi^{tt}_{\alpha\beta}\begin{pmatrix} l & l' \\ \kappa & \kappa' \end{pmatrix} = \sum_{\substack{k\in\kappa \\ k'\in\kappa'}} \phi_{\alpha\beta}\begin{pmatrix} l & l' \\ \kappa k & \kappa' k' \end{pmatrix} \tag{32a}$$

$$\phi^{tr}_{\alpha\beta}\begin{pmatrix} l & l' \\ \kappa & \kappa' \end{pmatrix} = \sum_{\substack{k\in\kappa \\ k'\in\kappa'}} \sum_{\gamma\delta} \phi_{\alpha\gamma}\begin{pmatrix} l & l' \\ \kappa k & \kappa' k' \end{pmatrix} \epsilon_{\gamma\beta\delta}\, X_\delta\,(k') \tag{32b}$$

$$\phi^{rt}_{\alpha\beta}\begin{pmatrix} l & l' \\ \kappa & \kappa' \end{pmatrix} = \sum_{\substack{k\in\kappa \\ k'\in\kappa'}} \sum_{\mu\nu} \phi_{\mu\beta}\begin{pmatrix} l & l' \\ \kappa k & \kappa' k' \end{pmatrix} \epsilon_{\mu\alpha\nu}\, X_\nu\,(k) \tag{32c}$$

and

$$\phi^{rr}_{\alpha\beta}\begin{pmatrix} l & l' \\ \kappa & \kappa' \end{pmatrix} = \sum_{\substack{k\in\kappa \\ k'\in\kappa'}} \sum_{\substack{\mu\nu \\ \gamma\delta}} \phi_{\mu\gamma}\begin{pmatrix} l & l' \\ \kappa k & \kappa' k' \end{pmatrix} \epsilon_{\mu\alpha\nu}\, \epsilon_{\gamma\beta\delta}\, X_\nu\,(k)\, X_\delta\,(k'). \tag{32d}$$

The interatomic force constants are to be obtained by differentiating the external short range potential given by (28), after ensuring that the short range potential along with Coulombic potential satisfies the constraint given by (25). The self terms $\phi\begin{pmatrix} o & o \\ \kappa & \kappa \end{pmatrix}$ are obtained by using the expressions (16a–d) given in § 6·3.

8. Application to α-KNO_3

8.1 *Refinement of parameters of the potential and calculation of phonon frequencies*

As already pointed out we have assumed a two-body potential of the type given by (23). We assumed that the effective charges in NO_3^- are as given by Pauling (1967) (see inset in figure (2)) namely that $O(1)$ is neutral, $O(2)$'s carry unit negative charges and the nitrogen carries unit positive charge. To maintain charge neutrality unit positive charge is associated with K^+. We assumed that the effective radii can be taken as those given by Kitaigorodsky and Mirskaya (1964) shown in table 6. With these charges and radii parameters we calculated the 'external' Coulombic

Table 6. Effective charges and radii parameters

Atom	Effective charge		Effective radius (Å)	
	Pauling's value	Equilibrium value	Kitaigorodsky's value	Equilibrium value
K	1·0	1·1	2·75	2·2
N	1·0	0·2	1·55	0·9
0(1)	0·0	−0·44	1·52	1·3
0(2)	−1·0	−0·43	1·52	1·3
Contribution to cohesive energy (eV)	−30·1	−34·6	19·1	0·6

and short range forces (eqs (27) and (29)) and also the contributions to the crystal cohesive energy per unit cell due to these interactions (eqs (26) and (28)). The resulting net forces on atoms were non-zero and some of them were quite large. Secondly the contribution to the cohesive energy due to the short range potential was much larger than the corresponding values for other ionic crystals like KCl.*

The dynamical matrix evaluated with the parameters discussed above was non-hermitean because the rotational sum rules were not being satisfied by those potential parameters. Forcing the dynamical matrix to be hermitean by arbitrarily equating the lower triangular part to the upper triangular part, and diagonalising such a matrix yielded nearly 50% of the frequencies to be imaginary for both the models.

Examination of the forces on the various atoms in the crystal indicated that K^+ ion was experiencing a large force due to the unequal charge distribution on the three oxygens of the NO_3^-. Hence the effective charges on the three oxygens were made equal**($\approx -0{\cdot}5$). The effective radii parameters were also reduced in order to bring down the contribution to the cohesive energy due to the short range forces†. The parameters were further allowed to change to minimise the forces but at the same time keeping the cohesive energy nearly the same. We evaluated the phonon frequencies at various stages of the parameter refinement and aimed at obtaining all phonon frequencies real. With the parameters as given in table 6 the rotational sum rules were almost satisfied and the resulting dynamical matrix for the model (ii) was also hermitean. This yielded real phonon frequencies. However, use of model (I) still resulted in nearly 30% of frequencies being imaginary. We find that the net forces on atoms cannot be reduced much further keeping the cohesive energy to be the same and therefore with model (I) we cannot obtain real frequencies only. Possible reasons of failure of model (I) not to yield real frequencies may be due to some of the reasons already discussed in § 7·4. In view of the simplicity of the model, we have not gone ahead with refinement of parameters once we get real frequencies in model (ii). There may be other sets of parameters which may yield real

*We have assumed in the absence of experimental data that the cohesive energy of KNO_3 is of the same order as that of other ionic crystals like KCl.

**In β- and γ-phase of potassium nitrate, the nitrate has a three fold symmetry. This justifies assuming equal charge distribution on the three oxygens.

†The Kitaigorodsky's radii may not be proper for two reasons. First, their values were not obtained for atoms in ionic solids and secondly they also included an attractive term (r^{-6}) in the proposed atom-atom potential.

frequencies and provide reasonable agreement with measured data as we have now. It is for this reason, use of constraints other than vanishing external forces was thought to be unnecessary at this stage of dynamical considerations of the solid.

8.2 *Use of group theory*

So far we have not discussed details of actual method of calculation of eigenfrequencies. We have made use of considerations given in § 6.4 extensively. The relevant result applicable to α-KNO_3 are discussed below.

We note that for $\mathbf{q}$ along Σ, $\triangle$ and Λ directions for all the elements S in $G_0(\mathbf{q})$, $S\mathbf{q}=\mathbf{q}$ or $-\mathbf{q}$. Thus in (19i) $\mathbf{G}=0$ and therefore

$$T^{ii'}_{\alpha\beta}(\kappa\kappa' \mid \mathbf{q}, S) = \delta_{ii'}\, c^i(S)\, S_{\alpha\beta}\, \delta[\kappa, F_0(\kappa' S)]. \tag{33}$$

Using the symmetry operations given in table 2, one can determine the permuted 'molecular' labels and thereby $\delta[\kappa, F_0(\kappa', S)]$. The latter decides the pair indices $\kappa\kappa'$ for which $\boldsymbol{T}(\kappa\kappa' \mid \mathbf{q}, S)$ will be non-zero. Table 7 gives the permuted molecular labels and the pair indices $\kappa\kappa'$ for which $\boldsymbol{T}(\kappa\kappa' \mid \mathbf{q}, S)$ are non-vanishing. Using (33) and table 7 one can easily construct $\boldsymbol{T}(\mathbf{q}, S)$. For example for $\mathbf{q}$ along Λ,

Table 7. (a) Permuted ' molecular ' lables under various space group operations

' Molecular ' lable (l=0) κ	Permuted ' molecular ' lable $\binom{l'}{\kappa'}$							
	S_1	S_2	S_3	S_4	S_5	S_6	S_7	S_8
1	0 0 0 1	1 0 0 3	−1 0−1 2	−1−1 0 4	−1−1−1 2	−1 0 0 4	0 0 0 1	1 0 0 3
2	0 0 0 2	0−1−1 4	−1 1−1 1	0−1 1 3	−1−1−1 1	0 1 1 3	0−1 0 2	0 0−1 4
3	0 0 0 3	0 0 0 1	−1 0−1 4	0−1 0 2	−1−1−1 4	0 0 0 2	0 0 0 3	0 0 0 1
4	0 0 0 4	1−1−1 2	−1 1−1 3	−1−1 1 1	−1−1−1 3	−1 1 1 1	0−1 0 4	1 0−1 2
5	0 0 0 5	0 0−1 7	−1 0−1 6	0−1 1 8	−1−1−1 6	0 0 1 8	0 0 0 5	0 0−1 7
6	0 0 0 6	1−1 0 8	−1 1−1 5	−1−1 0 7	−1−1−1 5	−1 1 0 7	0−1 0 6	1 0 0 8
7	0 0 0 7	1 0−1 5	−1 0−1 8	−1−1 1 6	−1−1−1 8	−1 0 1 6	0 0 0 7	1 0−1 5
8	0 0 0 8	0−1 0 6	−1 1−1 7	0−1 0 5	−1−1−1 7	0 1 0 5	0−1 0 8	0 0 0 6

The cell index l' is given in terms of three integers l'_1, l'_2, l'_3 corresponding to $X(l') = l'_1\, a\mathbf{i} + l'_2\, b\mathbf{j} + l'_3\, c\mathbf{k}$. $S_n = \{S_n/\mathbf{v}(S_n)\}$

Table 7. (b) Pair indices ($\kappa\kappa'$) for which $\delta(\kappa, F_0(\kappa', S))$ and therefore $T_{\alpha\beta}(\kappa\kappa' \mathbf{q}, R)$ are non vanishing

S_1	S_2	S_3	S_4	S_5	S_6	S_7	S_8
11	13	12	14	12	14	11	13
22	24	21	23	21	23	22	24
33	31	34	32	34	32	33	31
44	42	43	41	43	41	44	42
55	57	56	58	56	58	55	57
66	68	65	67	65	67	66	68
77	75	78	76	78	76	77	75
88	86	87	85	87	85	88	86

Table 8. The matrix $\boldsymbol{T}(\Lambda, R_2)$

$$
\begin{bmatrix}
0 & 0 & \boldsymbol{R}_2 & 0 & & & & & & & & & & & & \\
0 & 0 & 0 & \boldsymbol{R}_2 & & & & & & & & & & & & \\
\boldsymbol{R}_2 & 0 & 0 & 0 & & & 0 & & & & & 0 & & & & \\
0 & \boldsymbol{R}_2 & 0 & 0 & & & & & & & & & & & & \\
 & & & & & & & & & & \boldsymbol{R}_2 & 0 & 0 & 0 & & \\
 & & & & & & & & & & 0 & \boldsymbol{R}_2 & 0 & 0 & & \\
 & 0 & & & & & 0 & & & & 0 & 0 & \boldsymbol{R}_2 & \mathbf{0} & & \\
 & & & & & & & & & & 0 & 0 & 0 & \boldsymbol{R}_2 & & \\
 & & & & \boldsymbol{R}_2 & 0 & 0 & 0 & & & & & & & & \\
 & & & & 0 & \boldsymbol{R}_2 & 0 & 0 & & & & & & & & \\
 & 0 & & & 0 & 0 & \boldsymbol{R}_2 & 0 & & & & 0 & & & & \\
 & & & & 0 & 0 & 0 & \boldsymbol{R}_2 & & & & & & & &
\end{bmatrix}
$$

$\boldsymbol{R}_2 \in G_0(\Lambda)$, the $\boldsymbol{T}(\Lambda, R_2)$ is given in table 8. Using the $\boldsymbol{T}(\mathbf{q}, R)$ matrices the independent elements of the dynamical matrix are found to be [using (19h) and 19j)] $\boldsymbol{M}\begin{pmatrix}\mathbf{q}\\ \kappa\kappa'\end{pmatrix}$ with $\kappa\kappa' = 11, 12, 13, 14, 15, 16, 17, 18, 55, 56, 57$ and 58. These are the only elements we have evaluated in actual calculations.

The group of the wavevectors $G_0(\mathbf{q})$ and their IMRs (Kovalev 1964) for the three symmetry directions are given in table 4. Decomposition of $\boldsymbol{T}(\mathbf{q}, R)$ into various IMR's is also indicated therein. The symmetry vectors $\xi(q)$ were derived using the projection operator technique discussed in § 6.4. The symmetry vector matrices for the three symmetry directions are given in table 9. They were used to block diagonalise the dynamical matrix using the relation (22). The individual blocks obtained thereby were diagonalised by standard computer programmes. The phonon frequencies obtained from different blocks are labelled by the IMR to which the corresponding block belongs.

9. Results

Figure 8 shows the theoretical dispersion curves along the three symmetry directions, based on model (ii) described in § 7.4. In drawing these curves we have kept in view that the branches belonging to the same representation do not intersect. At points

Table 9a. Symmetry-adopted vector matrices for q along Σ, Δ and Λ directions*

$\xi(\Sigma)=1/\sqrt{2}$

	Σ_1										Σ_2										Σ_3										Σ_4									
$x(1)$	1	0	0	0	0	0	0	0	0	0	0	0	0	0	0	0	0	0	1	0	0	0	0	0	0	0	0	0	0	0	0	0	0	0	0	0	0	0	0	0	0	0
$y(1)$	0	0	0	0	0	0	0	0	0	0	1	0	0	0	0	0	0	0	0	0	0	0	0	0	0	0	0	0	0	1	0	0	0	0	0	0	0	0	0	0	0	0
$z(1)$	0	1	0	0	0	0	0	0	0	0	0	0	0	0	0	0	0	0	0	1	0	0	0	0	0	0	0	0	0	0	1	0	0	0	0	0	0	0	0	0	0	0
$x(2)$	0	0	1	0	0	0	0	0	0	0	0	0	0	0	0	0	0	0	0	0	1	0	0	0	0	0	0	0	0	0	0	1	0	0	0	0	0	0	0	0	0	0
$y(2)$	0	0	0	0	0	0	0	0	0	0	0	1	0	0	0	0	0	0	0	0	0	1	0	0	0	0	0	0	0	0	0	0	1	0	0	0	0	0	0	0	0	0
$z(2)$	0	0	0	1	0	0	0	0	0	0	0	0	0	0	0	0	0	0	0	0	0	0	1	0	0	0	0	0	0	0	0	0	0	1	0	0	0	0	0	0	0	0
$x(3)$	1	0	0	0	0	0	0	0	0	0	0	0	0	0	0	0	0	0	−1	0	0	0	0	0	0	0	0	0	0	0	0	0	0	0	1	0	0	0	0	0	0	0
$y(3)$	0	0	0	0	0	0	0	0	0	−1	0	0	0	0	0	0	0	0	0	0	0	0	0	0	0	0	0	0	0	0	0	0	0	0	0	1	0	0	0	0	0	0
$z(3)$	0	−1	0	0	0	0	0	0	0	0	0	0	0	0	0	0	0	0	0	1	0	0	0	0	0	0	0	0	0	0	0	0	0	0	0	0	1	0	0	0	0	0
$x(4)$	0	0	1	0	0	0	0	0	0	0	0	0	0	0	0	0	0	0	0	0	−1	0	0	0	0	0	0	0	0	0	0	0	0	0	0	0	0	1	0	0	0	0
$y(4)$	0	0	0	0	0	0	0	0	0	0	−1	0	0	0	0	0	0	0	0	0	0	1	0	0	0	0	0	0	0	0	0	0	0	0	0	0	0	0	1	0	0	0
$z(4)$	0	0	0	−1	0	0	0	0	0	0	0	0	0	0	0	0	0	0	0	0	0	0	1	0	0	0	0	0	0	0	0	0	0	0	0	0	0	0	0	1	0	0
$x(5)$	0	0	0	0	1	0	0	0	0	0	0	0	0	0	0	0	0	0	0	0	0	0	0	1	0	0	0	0	0	0	0	0	0	0	0	0	0	0	0	0	1	0
$y(5)$	0	0	0	0	0	0	0	0	0	0	0	1	0	0	0	0	0	0	0	0	0	0	0	0	1	0	0	0	0	0	0	0	0	0	0	0	0	0	0	0	0	0
$z(5)$	0	0	0	0	0	1	0	0	0	0	0	0	0	0	0	0	0	0	0	0	0	0	0	0	0	1	0	0	0	0	0	0	0	0	0	0	0	0	0	0	0	0
$\theta_x(5)$	0	0	0	0	0	0	0	0	0	0	0	0	1	0	0	0	0	0	0	0	0	0	0	0	0	0	1	0	0	0	0	0	0	0	0	0	0	0	0	0	0	0
$\theta_y(5)$	0	0	0	0	0	0	1	0	0	0	0	0	0	1	0	0	0	0	0	0	0	0	0	0	0	0	0	1	0	0	0	0	0	0	0	0	0	0	0	0	0	0
$\theta_z(5)$	0	0	0	0	0	0	0	0	0	0	0	0	0	0	1	0	0	0	0	0	0	0	0	0	0	0	0	0	1	0	0	0	0	0	0	0	0	0	0	0	0	0
$x(6)$	0	0	0	0	0	0	0	1	0	0	0	0	0	0	0	0	0	0	0	0	0	0	0	0	0	0	0	0	0	0	0	0	0	1	0	0	0	0	0	0	0	0
$y(6)$	0	0	0	0	0	0	0	0	0	0	0	0	0	0	0	1	0	0	0	0	0	0	0	0	0	0	0	0	0	0	0	0	0	0	1	0	0	0	0	0	0	0
$z(6)$	0	0	0	0	0	0	0	0	−1	0	0	0	0	0	0	0	0	0	0	0	0	0	0	0	0	0	0	0	0	0	0	0	0	0	0	1	0	0	0	0	0	0
$\theta_x(6)$	0	0	0	0	0	0	0	0	0	0	0	0	0	0	0	0	1	0	0	0	0	0	0	0	0	0	0	0	0	0	0	0	0	0	0	0	1	0	0	0	0	0
$\theta_y(6)$	0	0	0	0	0	0	0	0	0	−1	0	0	0	0	0	0	0	0	0	0	0	0	0	0	0	0	0	0	0	0	0	0	0	0	0	0	0	1	0	0	0	0
$\theta_z(6)$	0	0	0	0	0	0	0	0	0	0	0	0	0	0	0	0	0	1	0	0	0	0	0	0	0	0	0	0	0	0	0	0	0	0	0	0	0	0	1	0	0	0
$x(7)$	0	0	0	0	1	0	0	0	0	0	0	0	0	0	0	0	0	0	0	0	0	0	0	−1	0	0	0	0	0	0	0	0	0	0	0	0	0	0	0	1	0	0
$y(7)$	0	0	0	0	0	0	0	0	0	0	0	−1	0	0	0	0	0	0	0	0	0	0	0	0	1	0	0	0	0	0	0	0	0	0	0	0	0	0	0	0	1	0
$z(7)$	0	0	0	0	0	−1	0	0	0	0	0	0	0	0	0	0	0	0	0	0	0	0	0	0	0	1	0	0	0	0	0	0	0	0	0	0	0	0	0	0	0	0
$\theta_x(7)$	0	0	0	0	0	0	0	0	0	0	0	0	0	1	0	0	0	0	0	0	0	0	0	0	0	0	1	0	0	0	0	0	0	0	0	0	0	0	0	0	0	0
$\theta_y(7)$	0	0	0	0	0	0	−1	0	0	0	0	0	0	0	0	0	0	0	0	0	0	0	0	0	0	0	0	1	0	0	0	0	0	0	0	0	0	0	0	0	0	0
$\theta_z(7)$	0	0	0	0	0	0	0	0	0	0	0	0	0	0	−1	0	0	0	0	0	0	0	0	0	0	0	0	0	1	0	0	0	0	0	0	0	0	0	0	0	0	0
$x(8)$	0	0	0	0	0	0	0	1	0	0	0	0	0	0	0	0	0	0	0	0	0	0	0	0	0	0	0	0	0	−1	0	0	0	0	0	0	0	0	0	0	0	0
$y(8)$	0	0	0	0	0	0	0	0	0	0	0	0	0	0	0	−1	0	0	0	0	0	0	0	0	0	0	0	0	0	0	0	0	0	0	0	0	0	0	0	0	0	0
$z(8)$	0	0	0	0	0	0	0	0	1	0	0	0	0	0	0	0	0	0	0	0	0	0	0	0	0	0	0	0	0	0	1	0	0	0	0	0	0	0	0	0	0	0
$\theta_x(8)$	0	0	0	0	0	0	0	0	0	0	0	0	0	0	0	0	0	1	0	0	0	0	0	0	0	0	0	0	0	0	0	1	0	0	0	0	0	0	0	0	0	0
$\theta_y(8)$	0	0	0	0	0	0	0	0	0	1	0	0	0	0	0	0	0	0	0	0	0	0	0	0	0	0	0	0	0	0	0	0	1	0	0	0	0	0	0	0	0	0
$\theta_z(8)$	0	0	0	0	0	0	0	0	0	0	0	0	0	0	0	0	0	−1	0	0	0	0	0	0	0	0	0	0	0	0	0	0	0	1	0	0	0	0	0	0	0	0

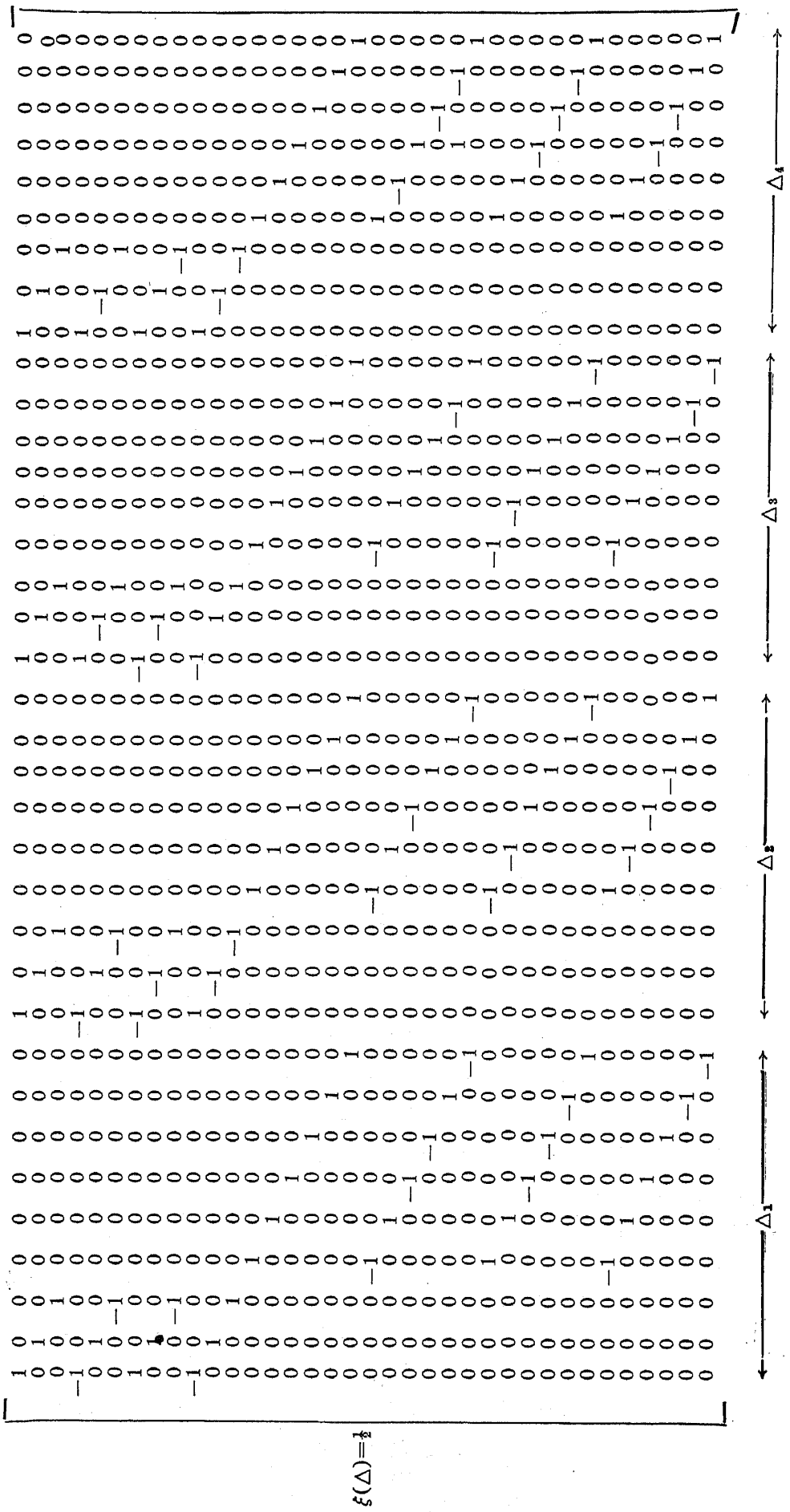

Table 9b.

Table 9(c).

$$\xi(\Lambda) = \frac{1}{\sqrt{2}}$$

1	0	0	0	0	0	0	0	0	0	0	0	0	0	0	0	0	0	0	0	0	0	0	0	0	0	1	0	0	0	0	0	0	0	0	0
0	0	0	0	0	0	0	0	0	0	1	0	0	0	0	0	0	0	1	0	0	0	0	0	0	0	0	0	0	0	0	0	0	0	0	0
0	1	0	0	0	0	0	0	0	0	0	0	0	0	0	0	0	0	0	0	0	0	0	0	0	0	0	1	0	0	0	0	0	0	0	0
0	0	1	0	0	0	0	0	0	0	0	0	0	0	0	0	0	0	0	0	0	0	0	0	0	0	0	0	1	0	0	0	0	0	0	0
0	0	0	0	0	0	0	0	0	0	0	1	0	0	0	0	0	0	0	1	0	0	0	0	0	0	0	0	0	0	0	0	0	0	0	0
0	0	0	1	0	0	0	0	0	0	0	0	0	0	0	0	0	0	0	0	0	0	0	0	0	0	0	0	0	1	0	0	0	0	0	0
0	0	−1	0	0	0	0	0	0	0	0	0	0	0	0	0	0	0	0	0	0	0	0	0	0	0	0	0	1	0	0	0	0	0	0	0
0	0	0	0	0	0	0	0	0	0	0	−1	0	0	0	0	0	0	0	1	0	0	0	0	0	0	0	0	0	0	0	0	0	0	0	0
0	0	0	1	0	0	0	0	0	0	0	0	0	0	0	0	0	0	0	0	0	0	0	0	0	0	0	0	0	−1	0	0	0	0	0	0
−1	0	0	0	0	0	0	0	0	0	0	0	0	0	0	0	0	0	0	0	0	0	0	0	0	0	1	0	0	0	0	0	0	0	0	0
0	0	0	0	0	0	0	0	0	0	−1	0	0	0	0	0	0	0	1	0	0	0	0	0	0	0	0	0	0	0	0	0	0	0	0	0
0	1	0	0	0	0	0	0	0	0	0	0	0	0	0	0	0	0	0	0	0	0	0	0	0	0	0	−1	0	0	0	0	0	0	0	0
0	0	0	0	1	0	0	0	0	0	0	0	0	0	0	0	0	0	0	0	0	0	0	0	0	0	0	0	0	0	1	0	0	0	0	0
0	0	0	0	0	0	0	0	0	0	0	0	1	0	0	0	0	0	0	0	1	0	0	0	0	0	0	0	0	0	0	0	0	0	0	0
0	0	0	0	0	1	0	0	0	0	0	0	0	0	0	0	0	0	0	0	0	0	0	0	0	0	0	0	0	0	0	1	0	0	0	0
0	0	0	0	0	0	0	0	0	0	0	0	0	1	0	0	0	0	0	0	0	1	0	0	0	0	0	0	0	0	0	0	0	0	0	0
0	0	0	0	0	0	1	0	0	0	0	0	0	0	0	0	0	0	0	0	0	0	0	0	0	0	0	0	0	0	0	0	1	0	0	0
0	0	0	0	0	0	0	0	0	0	0	0	0	0	1	0	0	0	0	0	0	0	1	0	0	0	0	0	0	0	0	0	0	0	0	0
0	0	0	0	0	0	0	1	0	0	0	0	0	0	0	0	0	0	0	0	0	0	0	0	0	0	0	0	0	0	0	0	0	1	0	0
0	0	0	0	0	0	0	0	0	0	0	0	0	0	0	1	0	0	0	0	0	0	0	1	0	0	0	0	0	0	0	0	0	0	0	0
0	0	0	0	0	0	0	0	1	0	0	0	0	0	0	0	0	0	0	0	0	0	0	0	0	0	0	0	0	0	0	0	0	0	1	0
0	0	0	0	0	0	0	0	0	0	0	0	0	0	0	0	1	0	0	0	0	0	0	0	1	0	0	0	0	0	0	0	0	0	0	0
0	0	0	0	0	0	0	0	0	1	0	0	0	0	0	0	0	0	0	0	0	0	0	0	0	0	0	0	0	0	0	0	0	0	0	1
0	0	0	0	0	0	0	0	0	0	0	0	0	0	0	0	0	1	0	0	0	0	0	0	0	1	0	0	0	0	0	0	0	0	0	0
0	0	0	0	0	0	0	−1	0	0	0	0	0	0	0	0	0	0	0	0	0	0	0	0	0	0	0	0	0	0	0	0	0	1	0	0
0	0	0	0	0	0	0	0	0	0	0	0	0	0	0	−1	0	0	0	0	0	0	0	1	0	0	0	0	0	0	0	0	0	0	0	0
0	0	0	0	0	0	0	0	1	0	0	0	0	0	0	0	0	0	0	0	0	0	0	0	0	0	0	0	0	0	0	0	0	0	−1	0
0	0	0	0	0	0	0	0	0	0	0	0	0	0	0	0	−1	0	0	0	0	0	0	0	1	0	0	0	0	0	0	0	0	0	0	0
0	0	0	0	0	0	0	0	0	−1	0	0	0	0	0	0	0	0	0	0	0	0	0	0	0	0	0	0	0	0	0	0	0	0	0	1
0	0	0	0	0	0	0	0	0	0	0	0	0	0	0	0	0	1	0	0	0	0	0	0	0	−1	0	0	0	0	0	0	0	0	0	0
0	0	0	0	−1	0	0	0	0	0	0	0	0	0	0	0	0	0	0	0	0	0	0	0	0	0	0	0	0	0	1	0	0	0	0	0
0	0	0	0	0	0	0	0	0	0	0	0	−1	0	0	0	0	0	0	0	1	0	0	0	0	0	0	0	0	0	0	0	0	0	0	0
0	0	0	0	0	1	0	0	0	0	0	0	0	0	0	0	0	0	0	0	0	0	0	0	0	0	0	0	0	0	0	−1	0	0	0	0
0	0	0	0	0	0	0	0	0	0	0	0	0	−1	0	0	0	0	0	0	0	1	0	0	0	0	0	0	0	0	0	0	0	0	0	0
0	0	0	0	0	0	−1	0	0	0	0	0	0	0	0	0	0	0	0	0	0	0	0	0	0	0	0	0	0	0	0	0	1	0	0	0
0	0	0	0	0	0	0	0	0	0	0	0	0	0	1	0	0	0	0	0	0	0	−1	0	0	0	0	0	0	0	0	0	0	0	0	0

←— Λ_1 —→ ←— Λ_2 —→ ←— Λ_3 —→ ←— Λ_4 —→

*The columns correspond to different representations as indicated at the bottom of each table.
The rows correspond to various linear and rotational displacements $x(r)$, $y(r)$, $z(r)$, $\theta_x(r)$, $\theta_y(r)$, $\theta_z(r)$; $r = 1......8$ of the different 'molecules' as indicated in (a).

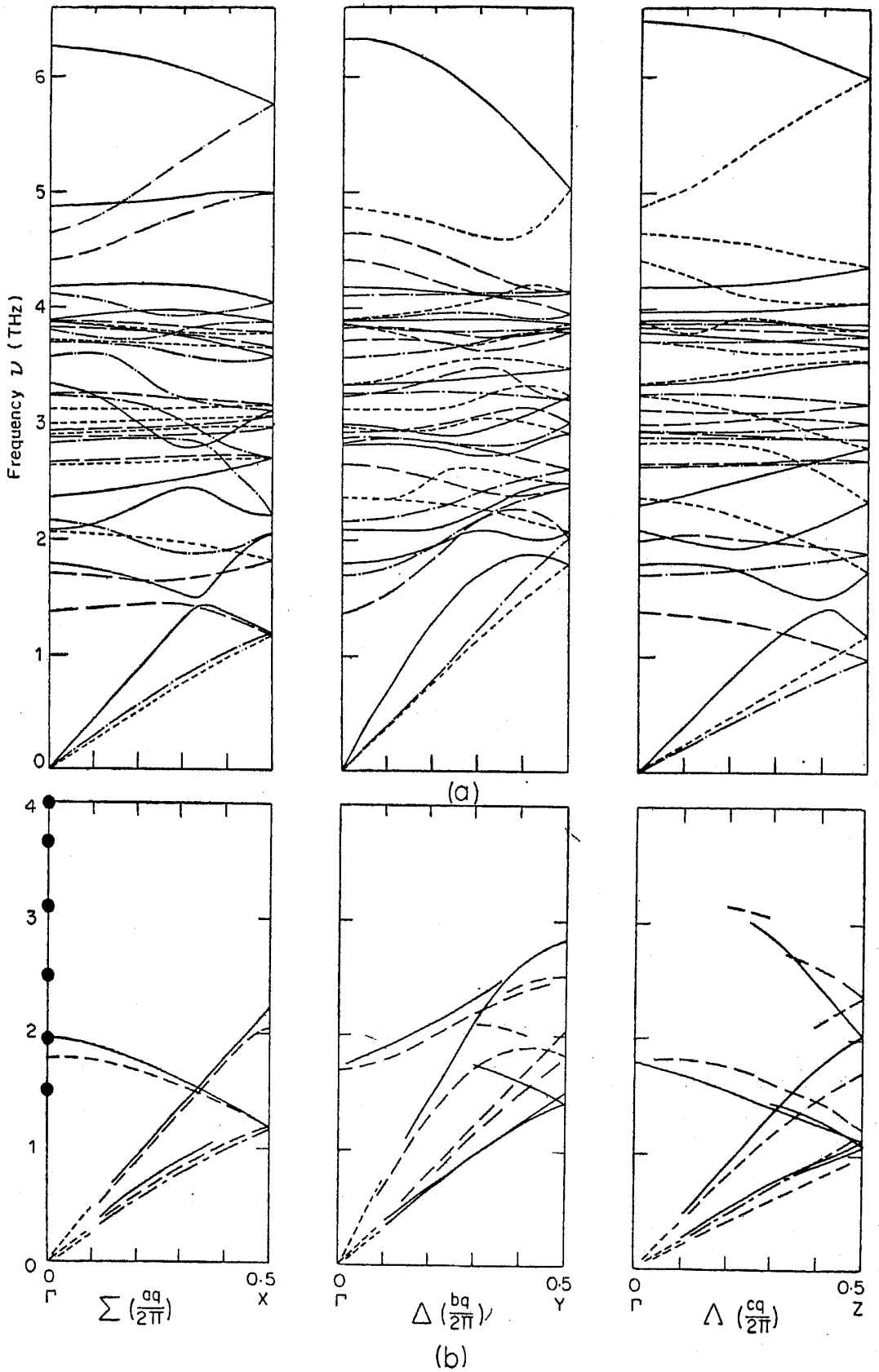

Figure 8a. Theoretical dispersion curves based on model (ii). The lines ——, – –, .–.–, - - - - correspond to first, second, third and fourth representations of $G_0(\mathbf{q})$ along the various **q**'s indicated.

Figure 8b. Resolution correlated dispersion curves—Continuous lines correspond to those derived from experimental data (Fig. 6) and dashed lines correspond to theoretical curves with which we believe the experimental curves are associated.

Table 10. Comparison of measured (Michard and Plicque 1971) and calculated elastic constants (units 10^{11} dynes cm^{-2})

Elastic constant	Measured	Derived from calculation q along		
		Σ	Δ	Λ
C_{11}	$3{\cdot}58 \pm 0{\cdot}04$		3·11	
C_{12}	$1{\cdot}34 \pm 0{\cdot}15$			
C_{13}	$1{\cdot}16 \pm 0{\cdot}15$			2·88
C_{22}	$3{\cdot}00 \pm 0{\cdot}03$			
C_{23}	$0{\cdot}92 \pm 0{\cdot}15$			
C_{33}	$2{\cdot}04 \pm 0{\cdot}02$	1·68		
C_{44}	$0{\cdot}67 \pm 0{\cdot}01$	0·72		0·80
C_{55}	$0{\cdot}54 \pm 0{\cdot}01$	0·63	0·87	
C_{66}	$0{\cdot}83 \pm 0{\cdot}01$		0·97	1·02
	$\rho = 2{\cdot}109$ g/cc			

X, Y and Z the branches degenerate in pairs due to higher symmetry of these points. (Table 4 indicates the compatibility of the branches at X, Y and Z). For comparison we have shown in figure 8 the resolution corrected experimental dispersion curves also. The continuous lines at the origin in this figure show the slopes of the dispersion curves based on elastic constant data (Michard and Plicque 1971). Comparison of the experimentally measured elastic constants and those derived from our theoretical calculations indicate remarkably good agreement as is seen in table 10. In the literature one finds that the elastic constants based on rigid ion model calculations are sometimes several times smaller or larger than measured values (for example see Striefer and Barsch, 1975). Continuous lines through resolution corrected frequencies give a guide to the eye of the experimental dispersion curves. We have also shown by dashed lines the theoretically calculated branches with which we believe the measured data are associated. Differences between the calculated and experimental dispersion curves are less than 15%. Frequencies obtained from experiments on laser Raman spectra (Balkanski, 1969, Bockermann *et al* 1976), are shown by concentric circles at $\mathbf{q}=0$. Although, several frequencies are indicated by Balkanski *et al* (1969), only two of the frequencies at 1·50 and 2·49 THz (1 THz = 33·3 cm^{-1}) are well confirmed by the recent work of Bockermann *et al* (1976). In the infrared spectrum also one observes only two frequencies at 2·4 and 3·9 THz (Hill and Mohan 1971).

We have also carried out inelastic neutron scattering measurements from a polycrystalline sample at room temperature using energy loss and energy gain techniques by means of filter detector spectrometer and a rotating crystal time-of-flight spectrometer. In the energy gain spectrum, a broad inelastic distribution is observed extending over 1·5 to 5 THz. No finer features like any singularities due to high density of states at any frequency could be discerned. The energy loss spectrum indicated an upper cut-off which is not more than 6·7 THz in the frequency distribution.

10. Summary

In this paper we have discussed the measurement and theoretical analysis of phonon dispersion curves of α-KNO_3 at room temperature. Group theoretical aid has been

extensively made use of in (a) choice of reciprocal lattice regions for measurements based on selection rules for neutron scattering and in (b) block diagonalisation of dynamical matrix, classification and labelling of phonon frequencies in terms of irreducible representations. The theory has made use of rigid molecular-ion model. Formalism based on external mode approach is resorted to for the first time in evaluating the Coulomb coefficients and short range interaction terms. The parameters defining the dynamical model were arrived at purely from the fact that the crystal is stable with the known structure and hence the equilibrium forces on atoms must be minimal in this configuration. The parameters have not been fitted to elastic or optic or neutron data and to this extent the calculations may be said to be even a kind of first-principle calculation. In view of this, the agreement between calculated values and measured data on elastic constants, optic frequencies and phonon dispersion relation may be said to be very satisfactory.

Acknowledgements

The authors have benefitted from several useful discussions with Dr V C Sahni. Dr S F Trevino has kindly made available the crystal and computer software for calculating group theoretical selection rules before its publication.

References

Balkanski M, Teng M K and Nusimovici M 1969 in *Light scattering spectra of solids* ed. G B Wright (New York: Springer-Verlag) p 731
Binbreck O S, Krishnamurthy N and Anderson 1974 *J. Chem. Phys.* **60** 4400
Bockermann H K, Sherman W F, Wilkinson G R and Mitra S S 1976 in *Molecular spectroscopy of dense phases* eds. M Grosmann, S G Elkomoss and J Ringeissen (Netherlands: Elsevier) p. 303
Born R C, Rohrer G A and Dhall B S 1970 *Proc. 20th Conf. electron components* p 149
Born M and Huang K 1954 *Dynamical theory of crystal lattices* (London, Oxford: Clarendon)
Bragg W L 1924 *Proc. Phys. Soc.* **A105** 16
Brockhouse B N 1960 *IAEA Symp. Vienna* p 113
Casella R C and Trevino S F 1972 *Phys. Rev.* **86** 4533
Chaplot S L 1978 Report BARC-972
Chen A and Chernow F 1967 *Phys. Rev.* **154** 493
Cochran W 1972 in *Proc. Int. School of Physics-Enrico Fermi-Course LII* ed. E Burstein p 345
Cooper M J and Nathans R 1967 *Acta Cryst.* **23** 357
Dolling G and Powell B M 1970 *Proc. R. Soc.* **319** 209
Dork R A, Schubring N W and Nolta J P 1964 *J. Appl. Phys.* **35** 1984
Doucet Y, Morabin A, Tete A and Rostini P 1965 *C. R. Acad. Sci. Paris* **261** 3060
Doucet Y, Morabin A, Tete A and Santini R 1966 *C. R. Acad. Sci. Paris* **263** 1286
Edwards D A 1931 *Z. Kristallogr. Kristallgeom.* **80** 154
Elliot R J and Thorpe M F 1967 *Proc. Phys. Soc. (London)* **91** 903
Ewald P P 1917 *Ann. Phys.* **54** 519 and 557
Gay J G 1967 in *Symposium on Ferroelectricity* held at General Motors Res. Lab. Warren, Michigan (Elsevier) p 161
Hill J C and Mohan P V 1971 *Ferroelectrics* **2** 201
Jona F and Shirane G 1962 *Ferroelectric Crystals* (New York: Pergamon)
Kellermann E W 1940 *Phil. Trans. R. Soc. (London)* **A238** 513
Kitaigorodsky A I and Mirskaya K V 1964 *Kristallografia* **9** 174

Kovalev O V 1964 *Irreducible representations of space groups* (New York: Gordon and Breach)
Krishnan R S and Haridasan T M 1972 *Indian J. Pure. Appl. Phys.* **10** 399
Mansingh A and Smith A M 1971 *J. Phys. D* (*Appl. Phys.*) **4** 1792
Maradudin A A and Vosko S H 1968 *Rev. Mod. Phys.* **40** 1
Michard F and Plicque F 1971 *Compt. Rend.* **B272** 848 and 1159
Nimmo J K and Lucas B W 1973 *J. Phys. C* (*Solid State Phys.*) **6** 201
Nolta J P, Schubring N W and Dork R A 1965 *J. Chem. Phys.* **42** 508
Nolta J P and Schubring N W 1962 *Phys. Rev. Lett.* **9** 285
Pauling L 1967 in *The Nature of the Chemical Bond and the Structure of Molecules and Crystals* (Calcutta: Oxford) p 283
Peckham G E, Saunderson D H and Sharp R I 1967 *Br. J. Appl. Phys.* **18** 473
Rafizadeh H A and Yip S 1970 *J. Chem. Phys.* **53** 315
Rapoport E and Kennedy G C 1965 *J. Phys. Chem. Solids* **26** 1995
Sakurai J, Coley R A and Dolling G 1970 *J. Phys. Soc. Jpn.* **28** 1426
Sawada S, Namura S and Asao Y 1961 *J. Phys. Soc.* (*Jpn.*) **16** 2486
Shinnaka Y 1962 *J. Phys. Soc.* (*Jpn.*) **17** 820
Siouffi J C and Cerisier P 1972 *Compt. Rend.* **B274** 754
Siouffi J C and Cerisier P 1972 *Compt. Rend.* **B275** 37
Slater J C 1965 *Quantum Theory of Molecules and Solids* (New York: McGraw Hill) Vol. 2
Striefer M E and Barsch G R 1975 *Phys. Rev.* **B12** 4553
Teng M K 1970 *Phys. Status Solidi* **40** 639
Teng M K, Balkanski M and Mourey J F 1971 *Solid State Commun.* **9** 465
Trevino S F, Farr M K, Gigurre P A and Aman J L 1976 in *Proc. of the Conf. on Neutron Scattering* (USA: Oak Ridge National Lab. A) Vol 1 p 152
Trevino S F, Prask H J and Casella R C 1974 *Phys. Rev.* **B10** 739
Trevino S F and Casella R C (unpublished)—private communication
Venkataraman G and Sahni V C 1970 *Rev. Mod. Phys.* **42** 409
Venkatesh A H 1978 BARC Report (to be published)
Wyckoff R W G 1925 *Am. J. Sci.* **9** 145
Wyckoff R W G 1964 in *Crystal Structure* II (New York: Interscience) p 365
Yanagi T and Sawada S 1963 *J. Phys. Soc. Jpn.* **18** 1228
Yanagi T 1965 *J. Phys. Soc. Jpn.* **20** 135